Molecular Therapy
Original Article

An Optimized Full-Length FLT3/CD3 Bispecific Antibody Demonstrates Potent Anti-leukemia Activity and Reversible Hematological Toxicity

Yik Andy Yeung,[1,9] Veena Krishnamoorthy,[1,9] Danielle Dettling,[1,4] Cesar Sommer,[1,5] Kris Poulsen,[1,5] Irene Ni,[1] Amber Pham,[1,6] Wei Chen,[1] Sindy Liao-Chan,[1,7] Kevin Lindquist,[1] S. Michael Chin,[1] Allison Given Chunyk,[3,8] Wenyue Hu,[2] Barbra Sasu,[1,5] Javier Chaparro-Riggers,[1] and Ivana Djuretic[1]

[1]Cancer Immunology Discovery, Oncology R&D, Pfizer Inc., South San Francisco, CA 94080, USA; [2]Drug Safety R&D, Pfizer Inc., San Diego, CA 94080, USA; [3]Biomedicine Design, Pfizer Inc., San Diego, CA 94080, USA

FLT3 (FMS-like tyrosine kinase 3), expressed on the surface of acute myeloid leukemia (AML) blasts, is a promising AML target, given its role in the development and progression of leukemia, and its limited expression in tissues outside the hematopoietic system. Small molecule FLT3 kinase inhibitors have been developed, but despite having clinical efficacy, they are effective only on a subset of patients and associated with high risk of relapse. A durable therapy that can target a wider population of AML patients is needed. Here, we developed an anti-FLT3-CD3 immunoglobulin G (IgG)-based bispecific antibody (7370) with a high affinity for FLT3 and a long half-life, to target FLT3-expressing AML blasts, irrespective of FLT3 mutational status. We demonstrated that 7370 has picomolar potency against AML cell lines *in vitro* and *in vivo*. 7370 was also capable of activating T cells from AML patients, redirecting their cytotoxic activity against autologous blasts at low effector-to-target (E:T) ratio. Additionally, under our dosing regimen, 7370 was well tolerated and exhibited potent efficacy in cynomolgus monkeys by inducing complete but reversible depletion of peripheral FLT3$^+$ dendritic cells (DCs) and bone marrow FLT3$^+$ stem cells and progenitors. Overall, our results support further clinical development of 7370 to broadly target AML patients.

INTRODUCTION

Acute myeloid leukemia (AML) is the most frequent acute leukemia in adults, yet it remains an area of high unmet medical need as standard therapy, including chemotherapy with or without allogeneic bone marrow transplantation has limited efficacy. The cure rate for adult patients who are 60 years of age or younger is 35% to 40%, and only 5% to 15% in patients who are older than 60.[1] Despite recent advances in understanding the disease heterogeneity and efforts in targeted molecular therapy, there remains an opportunity for an agent that targets a broad range of AML patients and results in complete and durable responses.[2,3]

FMS-like tyrosine kinase 3 (FLT3) is a class III receptor tyrosine kinase with a well-recognized and essential role in hematopoiesis.[4] It is expressed in human hematopoietic stem and progenitor cells (HSPCs), inducing their proliferation and differentiation into monocytes, dendritic cells (DCs), B cells, and T cells.[5,6] FLT3 expression in the mature human immune system remains largely limited to DCs. FLT3 also plays a key role in driving leukemogenesis and malignant progression of AML, promoting leukemic cell proliferation and survival.[7] Mutations in FLT3 resulting in constitutive activation of the receptor are commonly found in AML patients and are associated with poor prognosis and a high propensity to relapse after remission.[8,9] Overall, FLT3 signaling is a hallmark of both normal hematopoiesis and the development of AML.

FLT3 expression has been detected in almost all AML blasts and is generally higher than that on normal bone marrow HSPCs and circulating DCs.[10–12] The presence of an overexpressed oncogenic receptor on the surface of most leukemic blasts provides a unique opportunity for the development of antibody-based immunotherapies that would work in all AML patients irrespective of the FLT3 mutational status. Indeed, a monoclonal antibody targeting FLT3 (IMC-EB10) to drive antibody-dependent cell cytotoxicity (ADCC) has been developed and evaluated in the clinic.[13] However, likely due to the insufficient

Received 15 March 2019; accepted 27 December 2019;
https://doi.org/10.1016/j.ymthe.2019.12.014.

[4]Present address: Maverick Therapeutics Inc., Brisbane, CA 94002, USA

[5]Present address: Allogene Therapeutics Inc., South San Francisco, CA 94080, USA

[6]Present address: Acrus Bioscience Inc., Hayward, CA 94545, USA

[7]Present address: DistributedBio Inc., South San Francisco, CA 94080, USA

[8]Present address: Aptevo Therapeutics Inc., Seattle, WA 98121, USA

[9]These authors contributed equally to this work.

Correspondence: Yik Andy Yeung, Cancer Immunology Discovery, Oncology R&D, Pfizer Inc., South San Francisco, CA 94080, USA.
E-mail: yeungyik@yahoo.com
Correspondence: Javier Chaparro-Riggers, Cancer Immunology Discovery, Oncology R&D, Pfizer Inc., South San Francisco, CA 94080, USA.
E-mail: javier.chaparro-riggers@pfizer.com
Correspondence: Ivana Djuretic, Cancer Immunology Discovery, Oncology R&D, Pfizer Inc., South San Francisco, CA 94080, USA.
E-mail: ivanadj@hotmail.com

level of FLT3 surface expression to induce potent ADCC, clinical response was not observed.[14] Development of another antibody (4G8) with enhanced effector function was also recently described, but clinical activity has yet to be demonstrated.[15]

Alternatively, to enhance the elimination of AML cells, including those with a low level of FLT3 expression, T cell redirection, and chimeric antigen receptor (CAR) T cell-based therapies have also been pursued.[16–19] Using a mouse anti-human FLT3 4G8 antibody to construct a FLT3-CD3 bispecific antibody, Durben et al. demonstrated that the bispecific antibody can effectively redirect T cells to kill AML cell lines *in vitro* and *in vivo*; they also reported that the bispecific antibody can reduce patient AML blasts in assays with autologous T cells, albeit with most of the samples having high E:T ratio (>1:5).[16] Although the preclinical results were promising, FLT3 CD3 bispecific antibody described by Durben et al. may not have the most optimal characteristics as a therapeutic, namely because of short half-life and potentially higher immunogenicity risk associated with its mouse origin.[16] Meanwhile, CAR T cells targeting FLT3, derived from healthy donor T cells, could also efficiently mediate lysis of AML cell lines and patient AML blasts, but it remains unclear whether T cells from AML patients can be expanded sufficiently to generate autologous CAR T cells of equal potency.[20] One major concern for both of these T cell-based approaches is that, due to the expression of FLT3 on HSPCs, dose-dependent reductions of HSPCs have been observed *in vitro*.[15,18] However, the *in vivo* consequence of such potential on-target/off-tumor toxicity is not understood. It would be highly beneficial to determine whether myelosuppression or even myeloablation occurs following anti-FLT3-CD3 treatment in clinically relevant species.

When selecting a target for T cell redirection, important factors to consider are target expression in healthy tissues as well as the frequency of healthy cells expressing the target. Target expression in healthy tissues can contribute to immune-cell-mediated toxicity and limit the therapeutic dose that is required to mediate killing of cancer cells. FLT3 has very limited expression in normal tissues outside of bone marrow (Figure S1A).[15] In fact, comparison of the enrichment of target expression in AML compared to healthy non-hematopoietic tissues for FLT3 and three other commonly studied AML targets, CD33, CD123, and CLL1, suggested that agents targeting FLT3 may have the largest therapeutic index compared to agents targeting other AML targets. Blood, brain, pancreas, and lung are the top four healthy tissues expressing low levels of FLT3 RNA (Figure S1A). The expression of FLT3 protein in the brain was recently shown to be limited to the cytoplasm of Purkinje cells,[21] and the expression in the pancreas and lung tissue has not been confirmed at the level of cell surface protein expression.[15] Therefore, outside of potential hematological toxicities, FLT3-targeted T cell redirection therapies are expected to have little to no healthy tissue toxicity and present an opportunity to achieve therapeutic doses that are sufficiently high to mediate strong anti-tumor efficacy.

Here we describe the development of a human anti-FLT3 CD3 IgG-based bispecific antibody that was engineered to have a high affinity for FLT3 and a long half-life. We characterized its *in vitro* and *in vivo* efficacy using both AML cell lines and AML patient samples. We also evaluated its hematological toxicity in cynomolgus monkeys and show that it is reversible and potentially manageable in the clinical setting. The fully human IgG format with good manufacturability, long half-life, and high affinity for FLT3, as well as the choice of target make this bispecific antibody a very attractive clinical candidate with potential to induce durable remissions in AML patients.

RESULTS

Anti-FLT3 CD3 IgG-Based Bispecific Antibody Targeting Domain 4 Has the Most Optimal *In Vitro* and *In Vivo* Activity

A panel of human antibodies against human FLT3 was isolated using phage display technology. The binding epitopes of the antibodies were mapped to specific FLT3 extracellular domains using the truncation variants of FLT3 (Figure 1A; Figure S2). Representative antibodies targeting various domains of FLT3 were selected to pair with an anti-CD3 antibody to construct full-length bispecific antibodies (Figure 1B). Additional bispecific antibodies using previously described BV10 and 4G8 anti-FLT3 antibodies, which target domains 2 and 4 of FLT3, respectively, were also generated.[15] To compare the relative *in vitro* potency of these bispecific antibodies, we tested them in a cytotoxicity assay with a FLT3-expressing AML cell line EOL-1. Intriguingly, despite not having the highest affinity, domain 4 (D4)-targeting 4G8 bispecific antibody demonstrated the highest *in vitro* cytotoxicity, followed by mAb_E, which targets the most membrane proximal domain 5 (D5) (Figure 1C). The activities of 4G8 and mAb_E bispecifics were further compared in a subcutaneous AML (EOL-1) model in NOD scid gamma (NSG) mice. Figure 1D shows that although both bispecifics were efficacious in reducing tumor burden, 4G8 bispecific demonstrated much greater efficacy at 0.01 mg/kg dose, suggesting that domain 4 is likely to be the most optimal region for IgG-based bispecific targeting.

Properties of Domain 4-Targeting 7370 Anti-FLT3 CD3 Bispecific IgG

Additional human antibodies targeting FLT3 D4 were isolated and subsequently affinity matured to generate a lead clone. The engineered anti-FLT3 antibody was then paired with an anti-CD3 antibody (2B4) to generate the bispecific antibody 7370 (detailed biophysical characterization is shown in Figures S3A–S3D), which bound recombinant human FLT3 and CD3 proteins with dissociation constants of 49 pM and 27 nM, respectively (Figure S3E). In addition, 7370 demonstrated specific binding to human T cells, and AML cell lines EOL-1 and MV4-11 expressing high and low levels of FLT3, respectively (Figure S3F).[22] Epitope mapping studies indicated that binding of 7370 to FLT3 was abolished with an arginine substitution at D4 residue serine 370, confirming the 7370's binding specificity against FLT3 D4 (Figure S3G). The pharmacokinetic analysis of 7370 in NSG mice confirmed that 7370 had a terminal half-life of approximately 6 days (Figure S3H), in line with the half-lives of other typical human IgGs in mice. Similar half-life of approximately 6 days was also observed in cynomolgus monkeys (data not shown).

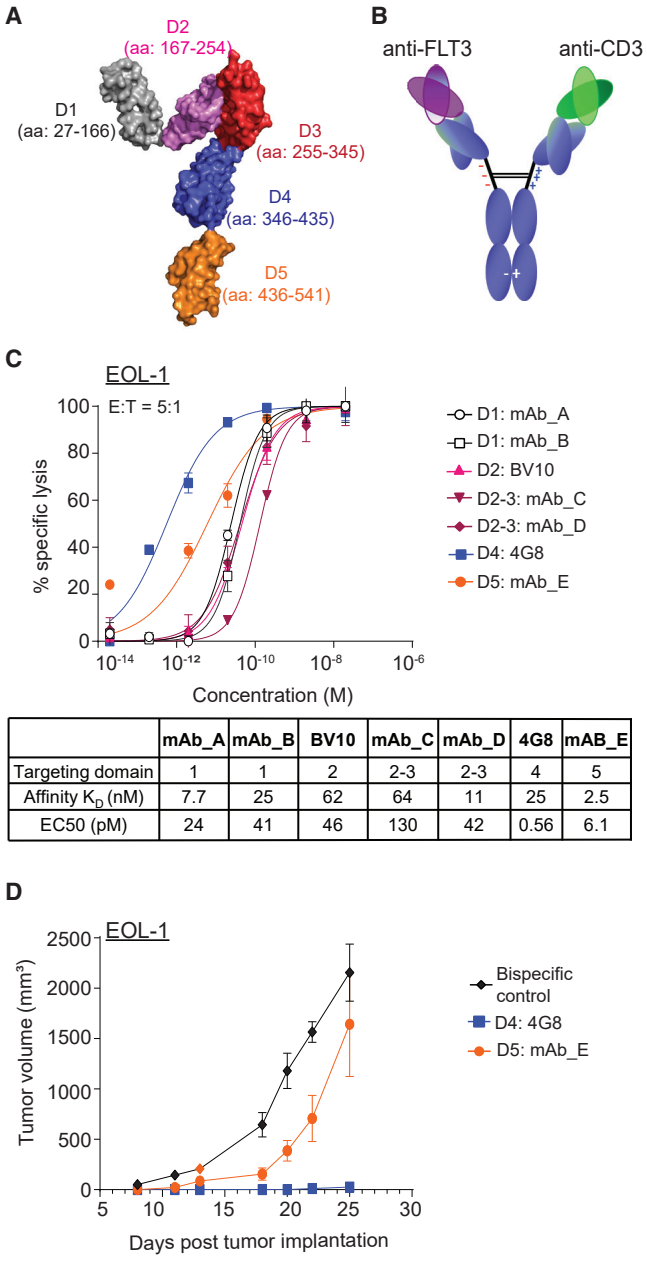

	mAb_A	mAb_B	BV10	mAb_C	mAb_D	4G8	mAB_E
Targeting domain	1	1	2	2-3	2-3	4	5
Affinity K_D (nM)	7.7	25	62	64	11	25	2.5
EC50 (pM)	24	41	46	130	42	0.56	6.1

Figure 1. Identification of Domain 4 of FLT3 as the Most Optimal Domain for IgG-Based Bispecific Antibody Targeting

(A) Structure of human FLT3 showing the domains 1 to 5 (D1–D5) of FLT3, modified from PDB: 3QS9 using PyMOL (Schrodinger). (B) Schematic representation of anti-FLT3-CD3 bispecific antibody. Bispecific IgGs were generated on the human IgG2ΔA backbone with D265A mutation (EU numbering) to abolish interactions with complement and Fcγ receptors. (C) *In vitro* cytotoxicity of healthy donor T cells against EOL-1 (E:T 5:1, 24 h assay) induced by FLT3-CD3 bispecific IgGs targeting different domains of FLT3. Table summarizes the binding affinity at 37°C for each bispecific antibody using surface plasmon resonance and calculated EC_{50} for cytotoxicity. Data shown are average ± SD. Data are representative of at least 2 donors. (D) Growth of s.c. implanted EOL-1 in NSG mice treated with 0.01 mg/kg 4G8 or mAb E FLT3-CD3 bispecific IgGs, targeting FLT3 D4 and D5, respectively (n = 10 mice per group). Data shown are average ± SEM. Data are representative of two studies with different donors. See also Figures S2 and S3.

7370 Anti-FLT3 CD3 Bispecific IgG Redirects Healthy Donor T Cells against AML Cell Lines with Picomolar Potency *In Vitro*

The activity of 7370 FLT3 bispecific antibody was then further characterized in the short-term cytotoxicity assay with healthy donor T cells and EOL-1 or MV4-11 AML cell lines (Figure 2). Maximal and near complete target cell lysis was observed at E:T ratio of 1:1, while substantial target cell lysis was detected at E:T ratios as low as 1:20 (Figures 2A and 2B). At E:T ratio of 1:20 (5% T cells), 7370 induced lysis of 33% of EOL-1 (Figure 2A) and 14% of MV4-11 (Figure 2B) cells. In this short-term cytotoxicity assay, lowering the E:T ratio affected only the maximal killing while the EC_{50}s did not appear substantially different. Likely, the capacity of individual T cells to mediate serial killing of targets presents a limitation for this short-term *in vitro* assay; therefore, E:T ratio of 1:1 was chosen to determine the *in vitro* potency of 7370 across multiple healthy donors.[23] At this ratio, 7370 redirected healthy donor T cells against AML cell lines at average EC_{50} of 1.4 ± 0.7 pM and 14.6 ± 5.6 pM for EOL-1 (Figure 2C) and MV4-11 (Figure 2D), respectively. Of note, no killing was induced by 7370 when a target cell line not expressing FLT3 was used (Figure S4). 7370 also potently induced interferon-γ (IFN-γ), tumor necrosis factor alpha (TNF-α), and interleukin-2 (IL-2) cytokines from healthy donor T cells in the presence of EOL-1 and MV4-11 cell lines (Figure S5).

The ability of 7370 to induce four activation markers on T cells, CD25, CD69, 41BB, and PD1 was also determined at E:T of 1:1 using EOL-1 as target cells. 7370 induced all four activation markers with similar single-digit pM potency (Figures 2E–2H; Figure S6). The kinetics of the induction of each activation marker were consistent with that described for antigen and T cell receptor (TCR)-mediated T cell activation; CD69 expression was transient, peaking at day 1, and decreasing thereafter; 41BB and PD1 induction was more sustained, peaking at day 2, decreasing slightly at day 3, and decreasing to baseline after 6 days; while CD25 stayed upregulated through day 6 of the culture, likely due to presence of cytokines secreted by activated T cells.[24–28] Therefore, 7370 induced transient T cell activation including the transient expression of the activation/exhaustion marker PD1.

Collectively, 7370 bispecific antibody potently redirected the cytotoxic and cytokine-secreting function of human T cells against cancer cells *in vitro*, accompanied by a transient induction of an activated state in T cells. The decrease in the expression of activation/exhaustion markers coincided with the complete elimination of tumor cells *in vitro*.

7370 Anti-FLT3 Bispecific IgG Is Efficacious in Established Orthotopic Xenograft Models of AML

To analyze the *in vivo* efficacy of 7370, we generated orthotopic AML xenograft models by IV injection of luciferase-labeled AML cell lines into NSG mice. Following the cell line engraftment, leukemia-bearing mice were first injected with previously activated and expanded human T cells (Figure S7) and subsequently treated with different doses of 7370 administered only once (Figure 3A).

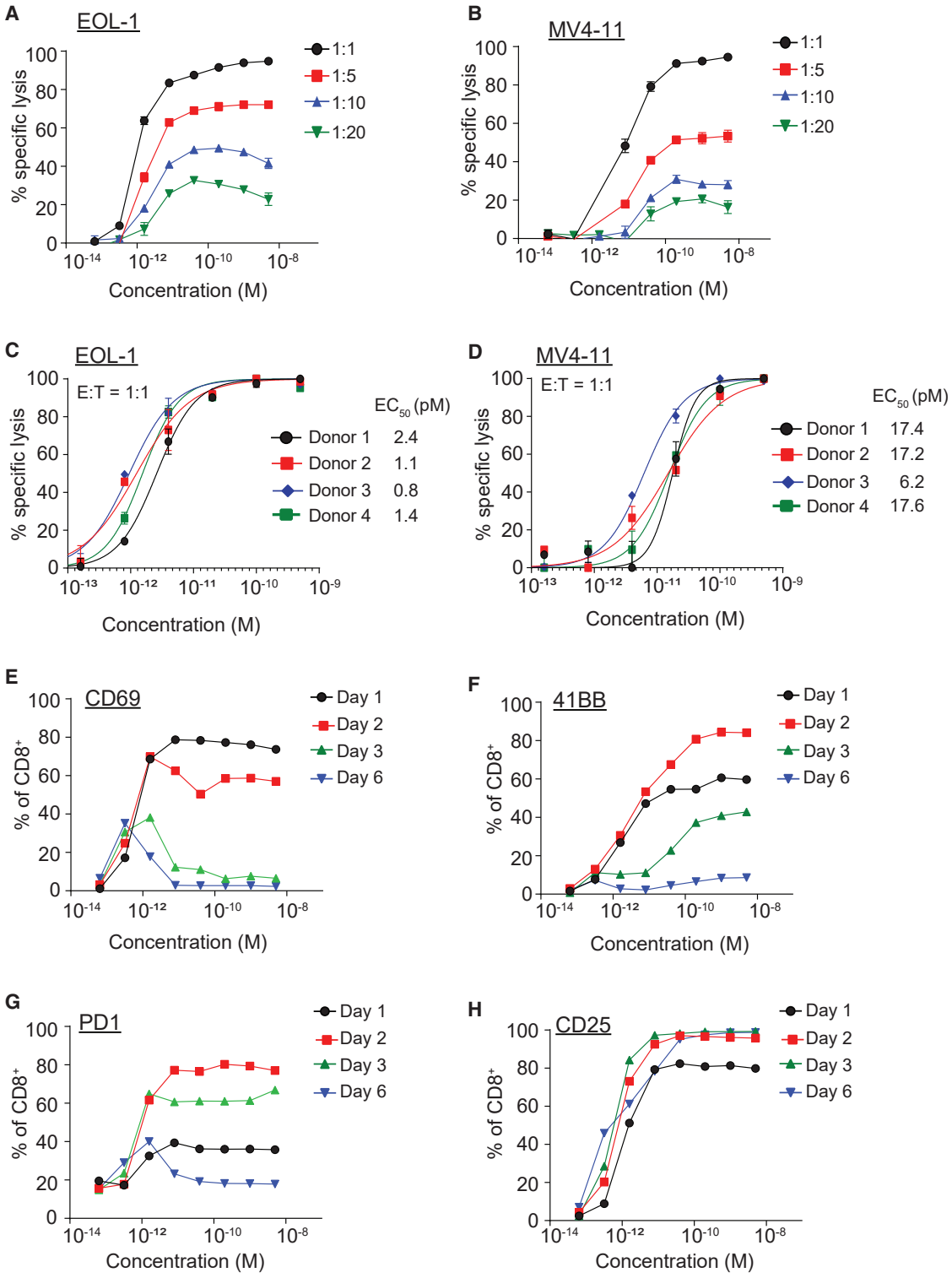

Figure 2. FLT3 Bispecific Mediates *In Vitro* Killing of AML Cell Lines at pM Potency

(A–D) Cytotoxicity induced by healthy donor T cells against luciferase-expressing EOL-1 (A and C) and MV4-11 (B and D) cells in the presence of 7370 for 2 days at different E:T ratios as depicted. Data shown are average ± SD. (E–H) Expression of activation markers CD69 (E), 41BB (F), PD1 (G), and CD25 (H) on healthy donor $CD8^+$ T cells at indicated time points after co-culture with EOL-1 (E:T 1:1) in the presence of 7370. Data in (A), (B), and (E)–(H) are representative of 2 donors. See also Figures S4–S6.

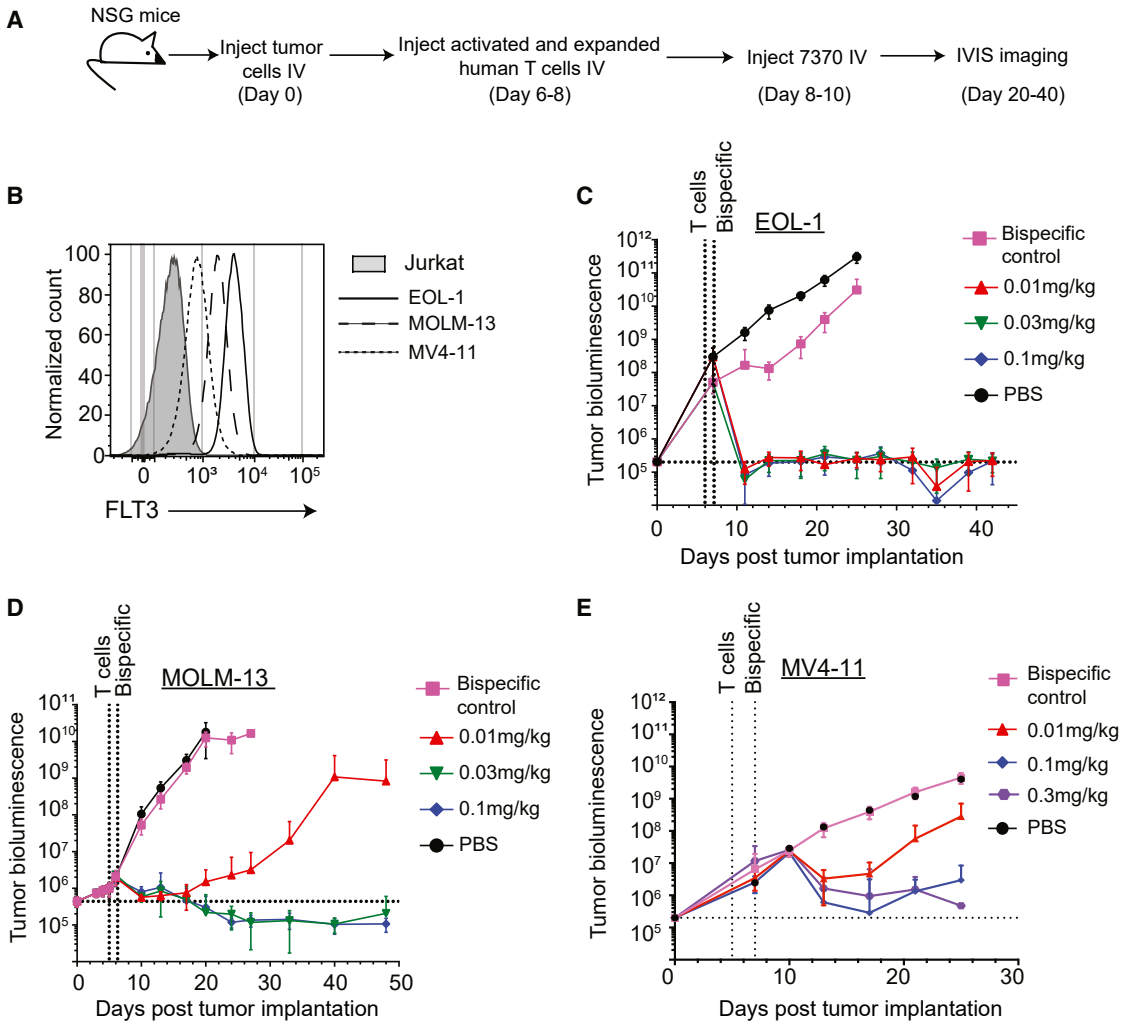

Figure 3. FLT3 Bispecific Is Highly Efficacious in Orthotopic Mouse Models of AML

(A) Experimental design for *in vivo* studies with 7370. (B) Surface expression of FLT3 on AML cell lines as indicated prior to injection into NSG mice. (C–E) Tumor growth as measured by bioluminescence imaging of EOL-1 (FLT3 wild-type) (C), MOLM-13 (FLT3-ITD) (D), and MV4-11 (FLT3-ITD) (E) in NSG mice, n = 10 per group. Data shown are average ± SEM. Data are representative of at least two studies per cell line. See also Figure S7.

To determine the effect of receptor density on *in vivo* efficacy of FLT3 bispecific antibody, we used three different cell lines for these studies, representing high (EOL-1), medium (MOLM-13), and low (MV4-11) levels of FLT3 antigen expression (Figures 3B–3E). In addition, we also chose these three cell lines in order to study representative FLT3 wild-type (EOL-1) and FLT3 mutant cell lines (MOLM-13 and MV4-11).[29,30] The results showed that a single dose of 7370 resulted in complete elimination of EOL-1 (Figure 3C) and MOLM-13 cells (Figure 3D) with 10 out of 10 mice remaining tumor-free for at least 40 days post tumor implantation. A lower dose of 7370 induced complete efficacy in the EOL-1 model than in the MOLM-13 model (0.01 mg/kg for EOL-1 and 0.03 mg/kg for MOLM-13), consistent with higher surface FLT3 expression on EOL-1 compared to MOLM-13. In the model with MV4-11, the cell line with the lowest FLT3 expression, a single dose of 7370 up to 0.3 mg/kg mediated significant reduction in tumor burden although it did not completely eliminate all AML cells (Figure 3E). Therefore, 7370 potently redirected human T cells against AML *in vivo* in a manner that was dependent on the expression of FLT3 antigen on AML cells but not on FLT3 mutational status.

7370 Anti-FLT3 Bispecific IgG Redirects AML Patient T Cells against Autologous AML Blasts

To determine whether AML patient T cells can be redirected against their own AML blasts in the presence of 7370, we obtained PBMCs from 5 AML patients with a substantial number of AML blasts present (Figure 4; Figure S8). E:T ratio calculated on the start of each culture (day 0) in these samples ranged from 1:25–1:64 and

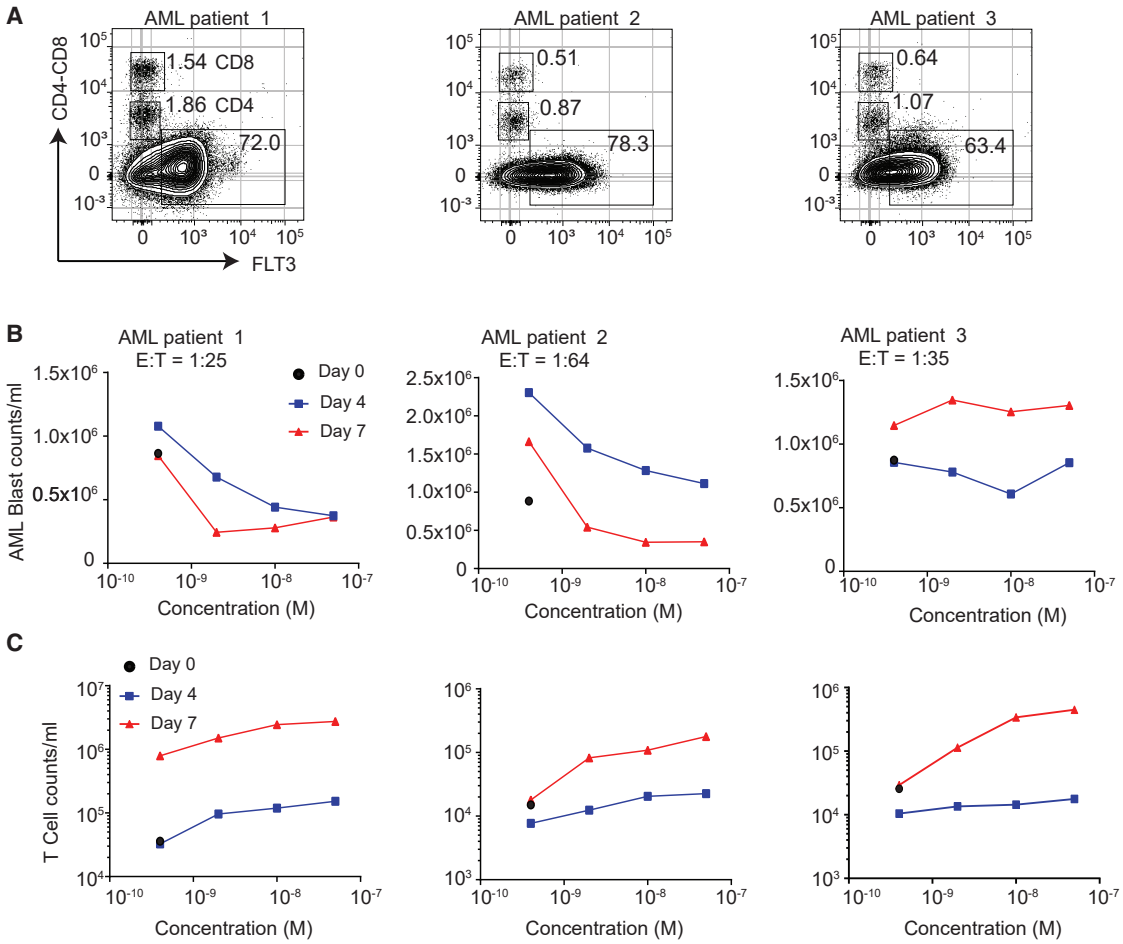

Figure 4. 7370 Anti-FLT3-CD3 IgG Redirects AML Patient T Cells against Autologous AML Blasts

(A) Flow cytometry plots depicting percent expression of FLT3 in PBMCs from 3 AML patients (x axis) and CD4 and CD8 markers (y axis). (B and C) Cell counts for AML blasts (B) and T cells (C) 0, 4, and 7 days after co-culture with 7370. E:T ratio was calculated for day 0 determined by identifying AML blasts as $CD45^{dim}CD3^{-}$, and T cells as sum of $CD45^{+}CD4^{+}$ and $CD45^{+}CD8^{+}$ T cells. See also Figure S8.

all expressed varying levels of FLT3 (Figure 4A; Figure S4A). Assessment of AML blast killing (Figure 4B; Figure S8B) and T cell proliferation (Figure 4C; Figure S8C) after up to 7 days in the presence of 7370 demonstrated that 7370 could redirect autologous T cells to proliferate and mediate cytotoxicity against autologous blasts. T cells from all 5 patients proliferated in a dose-dependent manner typically requiring 7370 at 0.5 nM or higher concentration. Furthermore, substantial cytotoxicity was induced in 4 out of 5 samples (Figure 4B; Figure S8B). Greater than 80% of blasts were depleted by day 7 for patients 1 and 2, while for patient 3 a maximum of ~35% decrease in blast counts was observed at day 4 and but no decrease at day 7. These data demonstrate that 7370 anti-FLT3 bispecific IgG was capable of activating AML patient T cells and inducing their cytotoxicity against autologous blasts, although in some cases AML blasts may be resistant to *in vitro* T cell killing even in the presence of FLT3 antigen expression.[15,31]

7370 Anti-FLT3 Bispecific IgG Is Well Tolerated in Cynomolgus Monkey at Doses that Achieve On-Target Efficacy with Reversible Hematological Toxicity

To study the pharmacology and tolerability of 7370 in cynomolgus monkey, we first demonstrated that it has reasonable cross-reactivity to cynomolgus FLT3 (Figure S9). We also confirmed that cynomolgus FLT3 was expressed in cynomolgus blood DCs and $CD34^{+}$ HSPCs in the bone marrow (Figures S10 and S11). FLT3 expression in cynomolgus and human blood immune cell subsets are similar (Figure S12). The cynomolgus study design is depicted in Figure 5A. Weekly doses of 3 mg/kg were administered twice to 4 monkeys as prior studies determined that 2 weekly doses as high as 0.9 mg/kg were tolerated (data not shown). Blood and bone marrow from 2 of 4 treated monkeys and 2 untreated controls were examined 2 days following the second dose of 7370. The remaining 2 treated monkeys were followed for an additional 2 weeks prior to study termination. This study design allowed us to assess both acute toxicity as well as the ability of treated

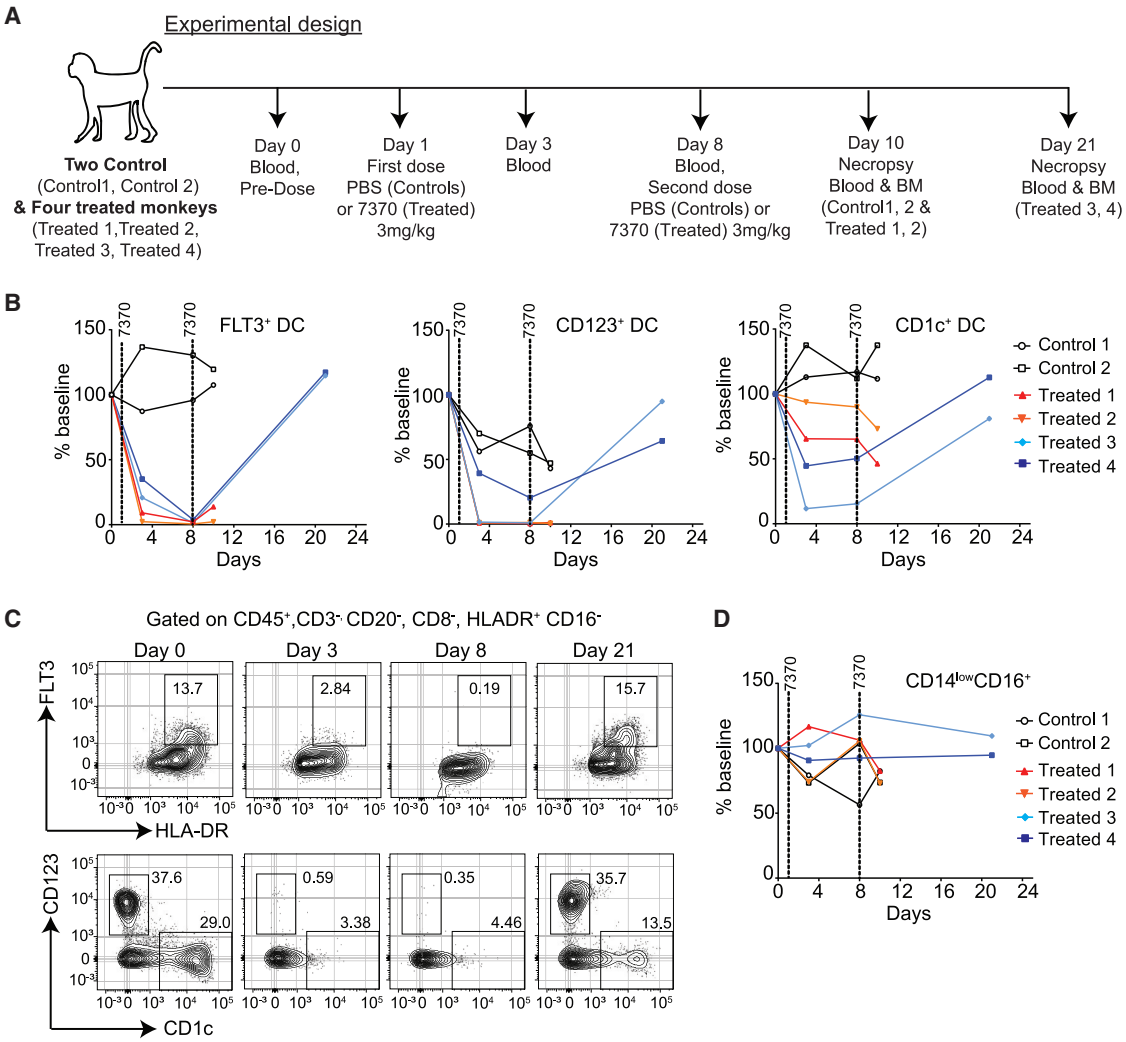

Figure 5. 7370 Anti-FLT3-CD3 IgG Induces Complete but Transient Depletion of Target Cells in Peripheral Blood of Cynomolgus Monkeys

(A) Experimental design and blood and bone marrow collection for the study. Blood was collected right before the first injection at day 1 (denoted as "day 0"). (B) Percentage of DC subsets: FLT3$^+$, CD123$^+$, and CD1c$^+$ in the blood of control and treated monkeys as indicated. Percent of baseline was calculated by dividing percent positive cells at indicated time point with that at baseline. (C) Flow cytometry plots showing FLT3$^+$ DCs (top panels) and CD123$^+$ and CD1c$^+$ DCs (bottom panels) for treated monkey 3 over the treatment and recovery period. DCs were identified by gating on lineage-negative cells as depicted in Figure S6. (D) Percentage of CD14^{low}CD16$^+$ cells in the blood of control and treated monkeys. See also Figures S9–S15.

monkeys to recover following discontinuation of treatment (Figure 5A).

The results showed that a near-complete depletion of FLT3$^+$ DCs, including the CD1c$^+$ and CD123$^+$ DC subsets, was observed 1 week after a single dose of 7370 (Figures 5B and 5C). The extent of depletion was in good agreement with the expression of FLT3 in different immune cell subsets in cynomolgus blood. CD14^{low}CD16$^+$ cells that don't express FLT3 (Figure S10) did not change during the treatment (Figure 5D). While DC depletion was maintained 2 days after the second dose, given a recovery period of additional 2 weeks, FLT3$^+$ DCs and CD1c$^+$ and CD123$^+$ DC subsets recovered to baseline levels (Figures 5B and 5C).

Decreases in blood immune subsets other than DCs were also detected 1 week following the first dose, most notably of B cells and monocytes, but all evaluated immune subsets returned back to baseline levels following the 2-week recovery period (Figures S13 and S14). Similarly, FLT3$^+$CD34$^+$CD38$^+$ HSPCs in the bone marrow were depleted in 2 treated monkeys analyzed 2 days following the second dose, but after the recovery period their percentage was similar to baseline in 1 monkey for which the tissue was available for analysis (Figure 6).

The pattern of cytokine release post treatment was in accordance with previously described CD3 bispecific studies.[32–34] An increase in IL-6, IL-10, and IFN-γ was observed after the first dose while no change in

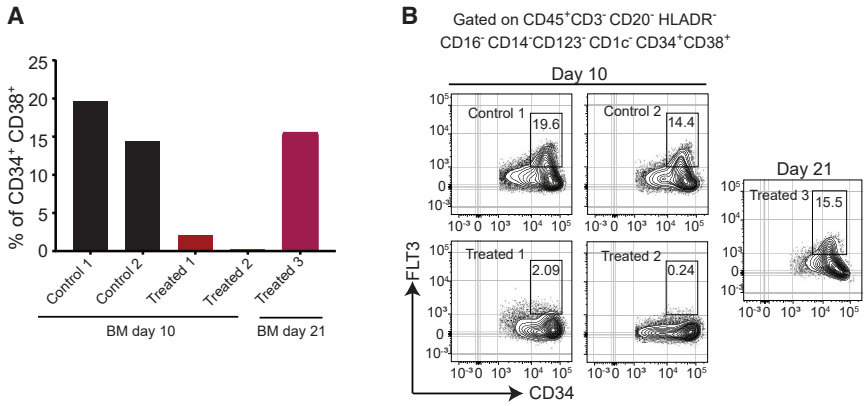

Figure 6. Anti-FLT3-CD3 IgG Induces Reversible Depletion of FLT3$^+$ HSPCs in Bone Marrow of Cynomolgus Monkeys

(A) Percentage of CD34$^+$CD38$^+$ HSPCs in the bone marrow of monkeys treated as depicted in Figure 5A. Lineage-negative cells were gated as depicted in Figure S7. (B) Flow cytometry plots showing the expression of FLT3 in CD34$^+$CD38$^+$ HSPCs in the bone marrow of all available monkeys at the terminal study time point. See also Figure S11.

cytokine levels was observed after the second dose (Figure S15). Only 1 out of 4 treated monkeys (treated 4) showed minimal clinical symptoms, including soft or liquid feces and body weight decreases of 0.92× of baseline at day 21. Microscopic findings in the monkeys included minimal to mild decreased cellularity in the bone marrow involving all components of hematopoiesis and minimal to moderate increased cellularity in the spleen and axillary lymph nodes. These findings were consistent with target-mediated depletion of FLT3-expressing cells and T cell activation. Examination of additional organs, including those that express FLT3 at the RNA level, such as brain, pancreas, and testes, demonstrated no changes to these organs by gross pathology and histopathology. Altogether, our results demonstrated that administration of two doses of 7370 resulted in a robust but transient FLT3$^+$ target cell elimination in both peripheral blood and the bone marrow without overt toxicities observed in other tissues.

DISCUSSION

We presented the preclinical characterization and toxicity assessment of a full-length IgG-based bispecific antibody targeting FLT3 for the treatment of AML. Although several other myeloid target antigens have been pursued in the context of CD3 bispecific antibodies for AML, including CD123, CD33, and CLL-1,[34–37] we chose to target FLT3 given its role as an oncogenic driver that is highly enriched in AML cells but has very limited expression in normal tissues outside of bone marrow (Figure S1A).[15] While brain, pancreas, and lung express low levels of FLT3 RNA (Figure S1A), the expression of FLT3 protein in the brain was recently shown to be limited to the cytoplasm of Purkinje cells,[21] and its expression in the pancreas and lung is lower than that of CD123 (Figure S1A). In the hematopoietic system, FLT3 expression is very limited in mature immune cells. Notably, the expression of FLT3 in mature myeloid cells, such as monocytes and neutrophils, was the lowest compared to other AML targets (Figure S1B). Consequently, CLL1-CD3 bispecific antibody treatment in cynomolgus monkeys resulted in neutrophil depletion,[34] whereas our studies showed that neutrophil counts in 7370-treated animals stay similar to those of untreated animals (Figure S14). Overall, the absence of a large off-tumor sink in healthy tissues should enable administration of higher doses of FLT3-CD3 bispecific antibody by minimizing the cytokine release syndrome and toxicities arising from on-target engagement in healthy tissues.

CD3 bispecific antibodies are promising therapeutics for cancer, exemplified by the success of the CD19-targeting BiTE, blinatumumab.[38] Here, we have fully optimized an IgG-based CD3 bispecific antibody against FLT3. First, we have carefully engineered the affinities of both FLT3 and CD3 targeting arms. The pM affinity of FLT3 antibody should allow the antibody to efficiently recognize low number of surface FLT3, estimated to be on the order of hundreds to low thousands,[15] and this is similar to a previously reported study on a CD3 bispecific modality targeting major histocompatibility complex (MHC)-peptide complex.[39] Also, the approximately 500-fold affinity difference between the FLT3 and CD3 targeting arms should allow preferential saturation of the FLT3 receptors over CD3, thereby avoiding any potential non-desirable T cell activation mediated by off-target binding of antibody-bound T cells. Second, we screened for and identified the FLT3 D4, instead of the membrane proximal D5, to be the most optimal region for our IgG-based bispecific antibody to target. Our results here are in contrast with previous studies suggesting that targeting the most membrane-proximal region of the receptor yielded the highest efficacy.[40,41] Such a difference is likely due to the distinctive binding geometry mediated by the unique structural fold of FLT3 and our IgG-based bispecific antibody, where such geometry is more favored in driving the proper synapse formation between T cells and AML cells.[42,43] This highlights the need to screen for a proper targeting region for individual formats of CD3 bispecific antibodies.[44] Lastly, we generated our bispecific antibody in full-length IgG format with abolished FcγR binding to have extended half-life (Figure S3H), to avoid non-specific T cell activation and to have favorable manufacturability. Such stable format enables a more convenient weekly or less frequent dosing regimen in the clinic without the need for continuous infusion.[15]

We demonstrated that 7370 was effective in redirecting autologous T cell in patients' samples to kill AML blasts, achieving more than 40% blast killing in 4 out of 5 samples after only 4 days in the presence of 10 nM of 7370. This extent of blast killing is in line with what has been reported for anti-CD33 BiTE.[45] In fact, Krupka et al.[45] showed

that for E:T between 1:10 and 1:80, a longer incubation (12–15 days) with the CD33 BiTE resulted in near complete blast killing *in vitro*, regardless of the CD33 expression level on AML blasts. Indeed, for patients 1 and 2, we also observed greater blast killing after 7 days, in particular for patient 2 (E:T = 1:64) for which complete elimination of the blasts was observed after 7 days of incubation with 7370.[45] Our study suggests that likely a nanomolar concentration of 7370 may be required in circulation to mediate substantial killing of the blasts through endogenous T cells, much higher than the picomolar EC_{50} observed for AML cell line killing by healthy T cells. This difference could be due to the lesser fitness of T cell in AML patients, low E:T ratio, and upregulation of immune checkpoints to resist killing.[20,31,35,45,46] Due to the limited expression of FLT3 in healthy tissues, such a high level of circulating drug concentration is potentially achievable for FLT3 bispecific antibody, as evidenced by the minimal toxicity observed for the 3 mg/kg dose administered in the cynomolgus study. Additionally, immune-modulating agents like anti-PD1/PDL1 antibodies[45] and cytokines[35] could potentially further enhance the effectiveness of the bispecific antibodies in the treatment of AML.

Because FLT3 is expressed in healthy HSPCs in the bone marrow, and, although AML blasts have been reported to have higher expression of FLT3 than healthy cells,[15,47,48] administration of FLT3 bispecific antibody at therapeutically relevant doses is likely to result in the depletion of healthy HSPCs and other cells expressing FLT3 such as DCs. We indeed observed depletion of $FLT3^+$ target cells in cynomolgus monkeys given 2 weekly doses of 7370 at a high dose level (3 mg/kg). Such a regimen was sufficient to deplete even $FLT3^+$ DCs that have been reported to have very low levels of surface FLT3 (<300 molecules/cell) in addition to $FLT3^+$ HSPCs in the bone marrow.[15] Not only was this dose level tolerable and did not induce any major clinical signs in treated monkeys, but the induced hematological toxicity was also not severe. We observed decreases in B cells and monocytes, although not as complete as with $FLT3^+$ DCs, that could be attributed to on-target effects. Furthermore, we also observed a reversibility of immune toxicities induced by this 2-dose regimen following a 2-week recovery period with both bone marrow and blood immune cells recovering to baseline. This suggests that it may be possible to manage hematological toxicity in the clinic by intermittent dosing in order to avoid severe myelosuppression and the need for allogeneic bone marrow transplantation. Potential combination with AML maintenance therapies could also be considered to avoid continuous dosing of FLT3 bispecific.

Unfortunately, no good preclinical models exist for studying the effects of long-term repeat dosing with FLT3 CD3 bispecific antibody. We have performed studies in the $CD34^+$ cell-humanized NSG-SGM3 model from The Jackson Laboratory (Bar Harbor, ME) and detected virtually no changes in the peripheral immune cell composition and numbers in time points after the administration of 7370 (data not shown). However, we could not detect FLT3 on the surface of human stem cells in the humanized NSG-SGM3 bone marrow to the same extent as on human HSCs *in vitro*, pointing at the challenges of using this model to conclude on the safety of FLT3-targeting agents (data not shown). On the other hand, the cyno model showed us that indeed FLT3 bispecific antibody could eliminate healthy cells expressing FLT3 and this is what is to be expected in the clinic, at least for patients with blasts that express similar levels of FLT3 as healthy stem cells (most patients express somewhat higher levels, though, as shown in Durben et al.[16]). Unfortunately, monkeys can develop anti-drug antibodies to human antibodies after 2–3 doses, and long-term repeat dosing may not be feasible. Future studies with surrogate anti-mouse FLT3 antibodies in human CD3-transgenic mouse models and/or with antibodies optimized for cynomolgous monkeys should be designed to further understand the effect of long-term dosing.

In conclusion, the robust anti-tumor activity of 7370 combined with good tolerability in cynomolgus monkeys, reversible hematological toxicity, and absence of non-hematological toxicity support its further clinical development in AML with carefully designed clinical dosing regimen to mitigate the potential for long-term hematopoietic toxicity risk. The FLT3 bispecific is potentially accessible to a broad AML population, irrespective of mutational status, while allowing for a safe and tolerable dosing regimen.

MATERIALS AND METHODS

Generation of the Recombinant FLT3 Antigens

Recombinant ectodomain of human FLT3 sequence and various truncation variants of FLT3 (Figure S2) with C-terminal histidine tag were synthesized by GeneArt (Thermo Fisher Scientific) and cloned into a CMV promotor-based expressing vector. Sequenced-verified vectors were then transfected into Expi293 cells for expression (Thermo Fisher Scientific). After 4–5 days of expression, the supernatant was purified over Ni Sepharose (GE Healthcare). Eluted proteins were further purified by size exclusion chromatography using a Superdex 200 column (GE Healthcare).

Isolation and Engineering of Anti-FLT3 Antibodies

A synthetic human single-chain Fv (scFv) phage library was used to isolate antibodies targeting FLT3. Four rounds of panning were performed against recombinant full-length human FLT3 according to a previously reported protocol.[49] FLT3 binding clones with unique sequences were then reformatted into human IgG expression vector. Human IgG were expressed using the Expi293 system (Thermo Fisher Scientific) and purified with MabSelect (GE Healthcare). The FLT3 binders were screened against recombinant full-length FLT3, and various FLT3 truncation variants (Figure S2) to map the binding domain of each antibody. D2-4 binders were further triaged by their ability to block commercially available FLT3 ligand (R&D Systems), BV10 antibody (anti-FLT3 D2 binders; Biolegend BV10A4H2), and 4G8 antibody (anti FLT3 D4 binders; BD Bioscience).

To isolate additional D4 binders, we constructed an antibody yeast display library using the antibody genes isolated from the ensemble phage library after the third round of panning. The yeast library was screened using 50–100 nM of recombinant hFLT3 D2-4. BV10-APC (Biolegend BV10A4H2) and anti-Cmyc-FITC (Thermo Fisher, 9E10) were used as the detection and normalization

antibodies, respectively. After three rounds of fluorescence-activated cell sorting (FACS) screening, individual yeast clones were cultured in 96-well plates, induced and incubated with hFLT3 D2-4. The binding of each clone was separately screened using two different detection antibodies, BV10-APC or 4G8-Alexa Fluor 647 (BD Bioscience). Selected clones were chosen for reformatting as human IgG for further characterization.

An anti-FLT3 lead clone mAb called P4H11 is chosen for affinity maturation using yeast display. The library was constructed by shuffling variable heavy region of P4H11 against human naive variable kappa light chains cloned from human donors. Four rounds of equilibrium based screening using biotinylated FLT3 with concentration starting from 20 nM down to 5 nM were performed. Two more rounds of kinetic-based screening were then carried out with cells being first labeled with 100 nM of biotinylated FLT3 and then followed by competition with 1 μM of free FLT3. Selected clones with unique sequences were reformatted as human IgG for affinity measurement.

Isolation and Engineering of Anti-CD3 Antibodies

The anti-CD3 antibody was generated using hybridoma technology. Briefly, BALB/c mice were immunized with keyhole limpet hemocyanin (KLH)-conjugated peptides representing the N-terminal residues 22–48 of human and cyno CD3 epilson. After repeated immunization and detectable serum titers against the immunogen, mouse spleens were harvested and fused with myeloma cells to generate hybridoma. Binding of the hybridoma antibodies were then screened against biotinylated human and cyno CD3 epilson peptides (residues 22–48), recombinant human and cyno CD3 epilson-delta (CD3εδ) protein. Antibodies were then further screened by their ability induce human and cynomolgus T cell proliferation. One clone, 2B4, was selected from the assay and subsequently humanized using conventional methods.

Generation of the Anti-FLT3/CD3 Bispecific Antibody

Anti-FLT3-CD3 hIgG2ΔA-based bispecific antibodies containing D265A were generated as previously described.[50] Briefly, anti-FLT3 antibody on the negatively charged (EEE) arm was exchanged with the anti-CD3 antibody on the positively charged (RRR) arm to generate the bispecific antibody.

Determination of Binding Affinities by Surface Plasmon Resonance

The affinities of antibodies binding to recombinant full-length FLT3 extracellular domain at 37°C were determined either using Biacore (GE LifeSciences) or ProteOn XPR36 SPR (BioRad). For characterization of 4G8 and BV10, a multi-cycle kinetics method was used on a Biacore T200 equipped with a CM4 sensor chip with anti-human Fc amine-coupled in all flow cells. The running and dilution buffer for the assay was PBS-TB (PBS, 0.05% Tween-20 (v/v), 1 mg/mL BSA, pH 7.4). Anti-FLT3 antibodies were first captured onto separate flow cells of the sensor chip at 0.75 μg/mL and a flow rate of 10 μL/min for 30 s. Antibody was not captured on flow cell 1 to serve as a reference surface. Recombinant FLT3 was then injected over all flow cells at 500 nM and 50 nM (in separate analysis cycles) for 2 min. Surfaces were regenerated with two 20 s injections of 75 mM phosphoric acid between analysis cycles. Sensorgrams were double-referenced and fit globally to the 1:1 Langmuir with mass transport model (K_D = koff/kon) using Biacore T200 Evaluation Software version 2.0.

Binding affinity for Req7370 was determined using a one-shot kinetic method on a ProteOn XPR36. Antibodies were first amine-coupled to the NLC sensor chip. Then, 2-fold dilutions of FLT3 from 10 nM to 0.62 nM in PBS-TB were injected for 3 min and dissociation was monitored for 2 h. Surfaces were regenerated with three 30 s injections of 2:1 (v/v) Pierce IgG Elution Buffer (Thermo Fisher): 4 M NaCl between analysis cycles. Sensorgrams were double-referenced and fit to a 1:1 Langmuir model using ProteOn Manager Software (version 3.1.0.6).

The affinities of antibodies binding to human recombinant CD3 at 37°C were determined using a multi-cycle kinetics method on a Biacore T200 equipped with CM4 sensor chip with anti-HIS antibody amine-coupled on all flow cells, using a running buffer of HBS-TB (10 mM HEPES, 150 mM NaCl, 0.05% Tween20, pH 7.4, 1 mg/mL BSA). In-house generated histidine-tagged human CD3εδ heterodimer protein was diluted in running buffer to 0.125 μg/mL and captured onto flow cell 2 of the sensor surface for 1 min at 10 μL/min. Then, bispecific antibodies from 300 nM to 4.7 nM (2-fold dilution series) were injected over flow cell 1 and 2 for 1 min and allowed to dissociate for 3 min. Surfaces were regenerated with two 30 s injections of 10 mM Glycine pH 1.7 between analysis cycles. Sensorgrams were double-fit to the 1:1 Langmuir with mass transport model using Biacore Evaluation Software version 2.0.

Cell Culture

EOL-1 cells were obtained from Sigma (St. Louis, MA), and MOLM-13 and MV4-11 cells were obtained from the American Type Culture Collection (ATCC) (Manassas, VA). AML cell lines were cultured in RPMI, 10% fetal bovine serum (FBS), penicillin-streptomycin at 37°C under 5% CO_2. Cells were engineered to express luciferase and GFP using Luc2AGFP lentivirus (AMSbio). Peripheral blood mononuclear cells (PBMCs) were isolated from blood obtained from healthy donors at Stanford Blood Center (Palo Alto, CA). Frozen PBMCs from AML patients were acquired from Fred Hutch (Seattle, MA). AML patient samples were thawed and rested for 4 h in SFEM II media (StemCell Technologies) after which they were supplemented with HSC expansion cocktail (CC110, StemCell Technologies). All experiments with patient samples were performed with appropriate consent.

In Vitro Cytotoxicity Assays

Cytotoxicity assays with AML cell lines were performed by mixing luciferase-expressing cell lines and purified human T cells. Cytotoxicity was assessed after 2 days (unless otherwise indicated) by measuring residual luciferase activity (One-Glo, Promega). Activation markers were detected by staining with antibodies against human CD45 (HI30), CD33 (WM53), CD4 (SK3), CD8 (SK1), CD25 (2A3), CD69 (FN50), 41BB (4B4-1), and PD-1 (EH12.2H7) and analyzed by flow cytometry.

For assays with AML patient samples, 7370 was added on day 0 and day 4 of the assay. Culture was also replenished with fresh SFEM II media and CC110 on day 4. AML blasts and T cells were identified by flow cytometry, and cell counts on day 4 and 7 calculated using counting beads (Thermo Fisher). The panel contained antibodies against the following: CD45 (HI30), CD33 (WM53), CD38 (HIT2), FLT3 (4G8), CD34 (8G12), CD4 (SK3), and CD8 (SK1). AML blasts were identified as $CD45^{low}CD3^{-}$.

AML Xenograft Models

Animal studies were carried out as per protocols approved by the Pfizer Animal Care and Use Committee. For subcutaneous (s.c.) screening models, bispecific antibodies were injected s.c. into NSG mice (Jackson) as indicated 1 day prior to injection with 1×10^6 EOL1 cells (s.c., in 50% growth-factor reduced Matrigel), and 2×10^6 freshly isolated human T cells intravenously (i.v.). Tumor growth was monitored by measuring tumor size.

For orthotopic models, luciferase-expressing AML cells were i.v. injected into NSG mice. After tumor engraftment (day 6–7), animals were administered 2×10^7 expanded human T cells (T cells purchased from Allcells; activated according to Miltenyi manufacturing protocol) by i.v. injection and 2 days later given either 7370 or a bispecific control antibody that lacks FLT3 binding in 100 μL of PBS. Tumor growth was monitored on the IVIS imager (Perkin Elmer).

Cynomolgus Monkey Studies

The study protocols for cynomolgus monkeys were approved by the Animal Care and Use Committee of the AAALAC certified institution. Blood and bone marrow were stained with antibodies against the following: CD3 (SP34.2), CD20 (2H7), HLADR (G46-6), CD8 (SK1), CD4 (SK3), CD16 (3G8), CD14 (M5E2), CD1c (L161), CD123 (7G3), CD49d (9F10), CD11c (3.9), FLT3 (BV10), CD45 (D058-1283), CD38 (AT-1), and CD34 (563).

SUPPLEMENTAL INFORMATION

Supplemental Information can be found online at https://doi.org/10.1016/j.ymthe.2019.12.014.

AUTHOR CONTRIBUTIONS

Y.A.Y., V.K., D.D., C.S., K.P., I.N., A.P., W.C., S.L.-C., K.L., and I.D. conducted the experiments and analyzed the results. W.H. and V.K. conducted and analyzed the toxicity study in cynomolgus monkeys. A.G.C. and V.K. conducted and analyzed the pharmacokinetic study. D.D., Y.A.Y., K.P., and J.C.-R. conceived the study. Y.A.Y., V.K., and I.D. wrote the manuscript, with help from the co-authors. Y.A.Y., B.S., J.C.-R., and I.D. supervised the work. All authors approved of the manuscript.

CONFLICTS OF INTEREST

At the time the study was conducted, all the authors were employees of Pfizer, which sponsored the study.

ACKNOWLEDGMENTS

We would like to thank the Biomedicine Design group at Pfizer La Jolla for performing the pharmacokinetic study. We also thank the protein expression and purification group, the vivarium, and the flow cytometry group at Pfizer South San Francisco for providing protein support, helping with animal studies, and helping with flow cytometry, respectively. We thank Edward Pascua and Carol Wang for their help with assays and analysis. We also thank Fred Hutchinson Cancer Research Center for providing access to primary AML samples. We thank David Shelton, Arvind Rajpal, Jaume Pons, Shu-Hui Liu, and Robert Rickert for support of this project. Funding is provided by Pfizer, Inc.

REFERENCES

1. Döhner, H., Weisdorf, D.J., and Bloomfield, C.D. (2015). Acute Myeloid Leukemia. N. Engl. J. Med. *373*, 1136–1152.
2. Larrosa-Garcia, M., and Baer, M.R. (2017). FLT3 Inhibitors in Acute Myeloid Leukemia: Current Status and Future Directions. Mol. Cancer Ther. *16*, 991–1001.
3. Medeiros, B.C., Fathi, A.T., DiNardo, C.D., Pollyea, D.A., Chan, S.M., and Swords, R. (2017). Isocitrate dehydrogenase mutations in myeloid malignancies. Leukemia *31*, 272–281.
4. Gilliland, D.G., and Griffin, J.D. (2002). The roles of FLT3 in hematopoiesis and leukemia. Blood *100*, 1532–1542.
5. Gabbianelli, M., Pelosi, E., Montesoro, E., Valtieri, M., Luchetti, L., Samoggia, P., Vitelli, L., Barberi, T., Testa, U., Lyman, S., et al. (1995). Multi-level effects of flt3 ligand on human hematopoiesis: expansion of putative stem cells and proliferation of granulomonocytic progenitors/monocytic precursors. Blood *86*, 1661–1670.
6. Ratajczak, M.Z., Ratajczak, J., Ford, J., Kregenow, R., Marlicz, W., and Gewirtz, A.M. (1996). FLT3/FLK-2 (STK-1) Ligand does not stimulate human megakaryopoiesis in vitro. Stem Cells *14*, 146–150.
7. Stirewalt, D.L., and Radich, J.P. (2003). The role of FLT3 in haematopoietic malignancies. Nat. Rev. Cancer *3*, 650–665.
8. Ley, T.J., Miller, C., Ding, L., Raphael, B.J., Mungall, A.J., Robertson, A., Hoadley, K., Triche, T.J., Jr., Laird, P.W., Baty, J.D., et al.; Cancer Genome Atlas Research Network (2013). Genomic and epigenomic landscapes of adult de novo acute myeloid leukemia. N. Engl. J. Med. *368*, 2059–2074.
9. Schnittger, S., Schoch, C., Dugas, M., Kern, W., Staib, P., Wuchter, C., Löffler, H., Sauerland, C.M., Serve, H., Büchner, T., et al. (2002). Analysis of FLT3 length mutations in 1003 patients with acute myeloid leukemia: correlation to cytogenetics, FAB subtype, and prognosis in the AMLCG study and usefulness as a marker for the detection of minimal residual disease. Blood *100*, 59–66.
10. Carow, C.E., Levenstein, M., Kaufmann, S.H., Chen, J., Amin, S., Rockwell, P., Witte, L., Borowitz, M.J., Civin, C.I., and Small, D. (1996). Expression of the hematopoietic growth factor receptor FLT3 (STK-1/Flk2) in human leukemias. Blood *87*, 1089–1096.
11. Rosnet, O., Bühring, H.J., Marchetto, S., Rappold, I., Lavagna, C., Sainty, D., Arnoulet, C., Chabannon, C., Kanz, L., Hannum, C., and Birnbaum, D. (1996). Human FLT3/FLK2 receptor tyrosine kinase is expressed at the surface of normal and malignant hematopoietic cells. Leukemia *10*, 238–248.
12. Armstrong, S.A., Mabon, M.E., Silverman, L.B., Li, A., Gribben, J.G., Fox, E.A., Sallan, S.E., and Korsmeyer, S.J. (2004). FLT3 mutations in childhood acute lymphoblastic leukemia. Blood *103*, 3544–3546.
13. Piloto, O., Nguyen, B., Huso, D., Kim, K.T., Li, Y., Witte, L., Hicklin, D.J., Brown, P., and Small, D. (2006). IMC-EB10, an anti-FLT3 monoclonal antibody, prolongs survival and reduces nonobese diabetic/severe combined immunodeficient engraftment of some acute lymphoblastic leukemia cell lines and primary leukemic samples. Cancer Res. *66*, 4843–4851.
14. Sanford, D., Blum, W.G., Ravandi, F., Klisovic, R.B., Borthakur, G., Walker, A.R., Garcia-Manero, G., Marcucci, G., Wierda, W.G., Whitman, S.P., et al. (2015). Efficacy and safety of an anti-FLT3 antibody (LY3012218) in patients with relapsed acute myeloid leukemia. J. of Clin. Oncol *33*, 7059.

15. Hofmann, M., Große-Hovest, L., Nübling, T., Pyż, E., Bamberg, M.L., Aulwurm, S., Bühring, H.J., Schwartz, K., Haen, S.P., Schilbach, K., et al. (2012). Generation, selection and preclinical characterization of an Fc-optimized FLT3 antibody for the treatment of myeloid leukemia. Leukemia *26*, 1228–1237.

16. Durben, M., Schmiedel, D., Hofmann, M., Vogt, F., Nübling, T., Pyz, E., Bühring, H.J., Rammensee, H.G., Salih, H.R., Große-Hovest, L., and Jung, G. (2015). Characterization of a bispecific FLT3 X CD3 antibody in an improved, recombinant format for the treatment of leukemia. Mol. Ther. *23*, 648–655.

17. Chen, L., Mao, H., Zhang, J., Chu, J., Devine, S., Caligiuri, M.A., and Yu, J. (2017). Targeting FLT3 by chimeric antigen receptor T cells for the treatment of acute myeloid leukemia. Leukemia *31*, 1830–1834.

18. Jetani, H., Garcia-Cadenas, I., Nerreter, T., Thomas, S., Rydzek, J., Meijide, J.B., Bonig, H., Herr, W., Sierra, J., Einsele, H., and Hudecek, M. (2018). CAR T-cells targeting FLT3 have potent activity against FLT3^{-}ITD^{+} AML and act synergistically with the FLT3-inhibitor crenolanib. Leukemia *32*, 1168–1179.

19. Wang, Y., Xu, Y., Li, S., Liu, J., Xing, Y., Xing, H., Tian, Z., Tang, K., Rao, Q., Wang, M., and Wang, J. (2018). Targeting FLT3 in acute myeloid leukemia using ligand-based chimeric antigen receptor-engineered T cells. J. Hematol. Oncol. *11*, 60.

20. Tasian, S.K. (2018). Acute myeloid leukemia chimeric antigen receptor T-cell immunotherapy: how far up the road have we traveled? Ther. Adv. Hematol. *9*, 135–148.

21. Çakmak-Görür, N., Radke, J., Rhein, S., Schumann, E., Willimsky, G., Heppner, F.L., Blankenstein, T., and Pezzutto, A. (2019). Intracellular expression of FLT3 in Purkinje cells: implications for adoptive T-cell therapies. Leukemia *33*, 1039–1043.

22. Reiter, K., Polzer, H., Krupka, C., Maiser, A., Vick, B., Rothenberg-Thurley, M., Metzeler, K.H., Dörfel, D., Salih, H.R., Jung, G., et al. (2018). Tyrosine kinase inhibition increases the cell surface localization of FLT3-ITD and enhances FLT3-directed immunotherapy of acute myeloid leukemia. Leukemia *32*, 313–322.

23. Hoffmann, P., Hofmeister, R., Brischwein, K., Brandl, C., Crommer, S., Bargou, R., Itin, C., Prang, N., and Baeuerle, P.A. (2005). Serial killing of tumor cells by cytotoxic T cells redirected with a CD19-/CD3-bispecific single-chain antibody construct. Int. J. Cancer *115*, 98–104.

24. Wen, T., Bukczynski, J., and Watts, T.H. (2002). 4-1BB ligand-mediated costimulation of human T cells induces CD4 and CD8 T cell expansion, cytokine production, and the development of cytolytic effector function. J. Immunol. *168*, 4897–4906.

25. Im, S.J., Hashimoto, M., Gerner, M.Y., Lee, J., Kissick, H.T., Burger, M.C., Shan, Q., Hale, J.S., Lee, J., Nasti, T.H., et al. (2016). Defining CD8+ T cells that provide the proliferative burst after PD-1 therapy. Nature *537*, 417–421.

26. Ahn, E., Araki, K., Hashimoto, M., Li, W., Riley, J.L., Cheung, J., Sharpe, A.H., Freeman, G.J., Irving, B.A., and Ahmed, R. (2018). Role of PD-1 during effector CD8 T cell differentiation. Proc. Natl. Acad. Sci. USA *115*, 4749–4754.

27. Sancho, D., Gómez, M., and Sánchez-Madrid, F. (2005). CD69 is an immunoregulatory molecule induced following activation. Trends Immunol. *26*, 136–140.

28. Sereti, I., Gea-Banacloche, J., Kan, M.Y., Hallahan, C.W., and Lane, H.C. (2000). Interleukin 2 leads to dose-dependent expression of the alpha chain of the IL-2 receptor on CD25-negative T lymphocytes in the absence of exogenous antigenic stimulation. Clin. Immunol. *97*, 266–276.

29. Quentmeier, H., Reinhardt, J., Zaborski, M., and Drexler, H.G. (2003). FLT3 mutations in acute myeloid leukemia cell lines. Leukemia *17*, 120–124.

30. Zheng, R., Levis, M., Piloto, O., Brown, P., Baldwin, B.R., Gorin, N.C., Beran, M., Zhu, Z., Ludwig, D., Hicklin, D., et al. (2004). FLT3 ligand causes autocrine signaling in acute myeloid leukemia cells. Blood *103*, 267–274.

31. Laszlo, G.S., Gudgeon, C.J., Harrington, K.H., and Walter, R.B. (2015). T-cell ligands modulate the cytolytic activity of the CD33/CD3 BiTE antibody construct, AMG 330. Blood Cancer J. *5*, e340.

32. Teachey, D.T., Rheingold, S.R., Maude, S.L., Zugmaier, G., Barrett, D.M., Seif, A.E., Nichols, K.E., Suppa, E.K., Kalos, M., Berg, R.A., et al. (2013). Cytokine release syndrome after blinatumomab treatment related to abnormal macrophage activation and ameliorated with cytokine-directed therapy. Blood *121*, 5154–5157.

33. Chichili, G.R., Huang, L., Li, H., Burke, S., He, L., Tang, Q., Jin, L., Gorlatov, S., Ciccarone, V., Chen, F., et al. (2015). A CD3xCD123 bispecific DART for redirecting host T cells to myelogenous leukemia: preclinical activity and safety in nonhuman primates. Sci. Transl. Med. *7*, 289ra82.

34. Leong, S.R., Sukumaran, S., Hristopoulos, M., Totpal, K., Stainton, S., Lu, E., Wong, A., Tam, L., Newman, R., Vuillemenot, B.R., et al. (2017). An anti-CD3/anti-CLL-1 bispecific antibody for the treatment of acute myeloid leukemia. Blood *129*, 609–618.

35. Al-Hussaini, M., Rettig, M.P., Ritchey, J.K., Karpova, D., Uy, G.L., Eissenberg, L.G., Gao, F., Eades, W.C., Bonvini, E., Chichili, G.R., et al. (2016). Targeting CD123 in acute myeloid leukemia using a T-cell-directed dual-affinity retargeting platform. Blood *127*, 122–131.

36. Aigner, M., Feulner, J., Schaffer, S., Kischel, R., Kufer, P., Schneider, K., Henn, A., Rattel, B., Friedrich, M., Baeuerle, P.A., et al. (2013). T lymphocytes can be effectively recruited for ex vivo and in vivo lysis of AML blasts by a novel CD33/CD3-bispecific BiTE antibody construct. Leukemia *27*, 1107–1115.

37. Reusch, U., Harrington, K.H., Gudgeon, C.J., Fucek, I., Ellwanger, K., Weichel, M., Knackmuss, S.H., Zhukovsky, E.A., Fox, J.A., Kunkel, L.A., et al. (2016). Characterization of CD33/CD3 Tetravalent Bispecific Tandem Diabodies (TandAbs) for the Treatment of Acute Myeloid Leukemia. Clin. Cancer Res. *22*, 5829–5838.

38. Bargou, R., Leo, E., Zugmaier, G., Klinger, M., Goebeler, M., Knop, S., Noppeney, R., Viardot, A., Hess, G., Schuler, M., et al. (2008). Tumor regression in cancer patients by very low doses of a T cell-engaging antibody. Science *321*, 974–977.

39. Liddy, N., Bossi, G., Adams, K.J., Lissina, A., Mahon, T.M., Hassan, N.J., Gavarret, J., Bianchi, F.C., Pumphrey, N.J., Ladell, K., et al. (2012). Monoclonal TCR-redirected tumor cell killing. Nat. Med. *18*, 980–987.

40. Li, J., Stagg, N.J., Johnston, J., Harris, M.J., Menzies, S.A., DiCara, D., Clark, V., Hristopoulos, M., Cook, R., Slaga, D., et al. (2017). Membrane-Proximal Epitope Facilitates Efficient T Cell Synapse Formation by Anti-FcRH5/CD3 and Is a Requirement for Myeloma Cell Killing. Cancer Cell *31*, 383–395.

41. Bluemel, C., Hausmann, S., Fluhr, P., Sriskandarajah, M., Stallcup, W.B., Baeuerle, P.A., and Kufer, P. (2010). Epitope distance to the target cell membrane and antigen size determine the potency of T cell-mediated lysis by BiTE antibodies specific for a large melanoma surface antigen. Cancer Immunol. Immunother. *59*, 1197–1209.

42. Davis, S.J., and van der Merwe, P.A. (2006). The kinetic-segregation model: TCR triggering and beyond. Nat. Immunol. *7*, 803–809.

43. Verstraete, K., Vandriessche, G., Januar, M., Elegheert, J., Shkumatov, A.V., Desfosses, A., Van Craenenbroeck, K., Svergun, D.I., Gutsche, I., Vergauwen, B., and Savvides, S.N. (2011). Structural insights into the extracellular assembly of the hematopoietic Flt3 signaling complex. Blood *118*, 60–68.

44. Velasquez, M.P., Bonifant, C.L., and Gottschalk, S. (2018). Redirecting T cells to hematological malignancies with bispecific antibodies. Blood *131*, 30–38.

45. Krupka, C., Kufer, P., Kischel, R., Zugmaier, G., Lichtenegger, F.S., Köhnke, T., Vick, B., Jeremias, I., Metzeler, K.H., Altmann, T., et al. (2016). Blockade of the PD-1/PD-L1 axis augments lysis of AML cells by the CD33/CD3 BiTE antibody construct AMG 330: reversing a T-cell-induced immune escape mechanism. Leukemia *30*, 484–491.

46. Harrington, K.H., Gudgeon, C.J., Laszlo, G.S., Newhall, K.J., Sinclair, A.M., Frankel, S.R., Kischel, R., Chen, G., and Walter, R.B. (2015). The Broad Anti-AML Activity of the CD33/CD3 BiTE Antibody Construct, AMG 330, Is Impacted by Disease Stage and Risk. PLoS ONE *10*, e0135945.

47. Kuchenbauer, F., Kern, W., Schoch, C., Kohlmann, A., Hiddemann, W., Haferlach, T., and Schnittger, S. (2005). Detailed analysis of FLT3 expression levels in acute myeloid leukemia. Haematologica *90*, 1617–1625.

48. Kindler, T., Lipka, D.B., and Fischer, T. (2010). FLT3 as a therapeutic target in AML: still challenging after all these years. Blood *116*, 5089–5102.

49. Yeung, Y.A., Foletti, D., Deng, X., Abdiche, Y., Strop, P., Glanville, J., Pitts, S., Lindquist, K., Sundar, P.D., Sirota, M., et al. (2016). Germline-encoded neutralization of a Staphylococcus aureus virulence factor by the human antibody repertoire. Nat. Commun. *7*, 13376.

50. Strop, P., Ho, W.H., Boustany, L.M., Abdiche, Y.N., Lindquist, K.C., Farias, S.E., Rickert, M., Appah, C.T., Pascua, E., Radcliffe, T., et al. (2012). Generating bispecific human IgG1 and IgG2 antibodies from any antibody pair. J. Mol. Biol. *420*, 204–219.

YMTHE, Volume *28*

Supplemental Information

An Optimized Full-Length FLT3/CD3 Bispecific Antibody Demonstrates Potent Anti-leukemia Activity and Reversible Hematological Toxicity

Yik Andy Yeung, Veena Krishnamoorthy, Danielle Dettling, Cesar Sommer, Kris Poulsen, Irene Ni, Amber Pham, Wei Chen, Sindy Liao-Chan, Kevin Lindquist, S. Michael Chin, Allison Given Chunyk, Wenyue Hu, Barbra Sasu, Javier Chaparro-Riggers, and Ivana Djuretic

Figure S1

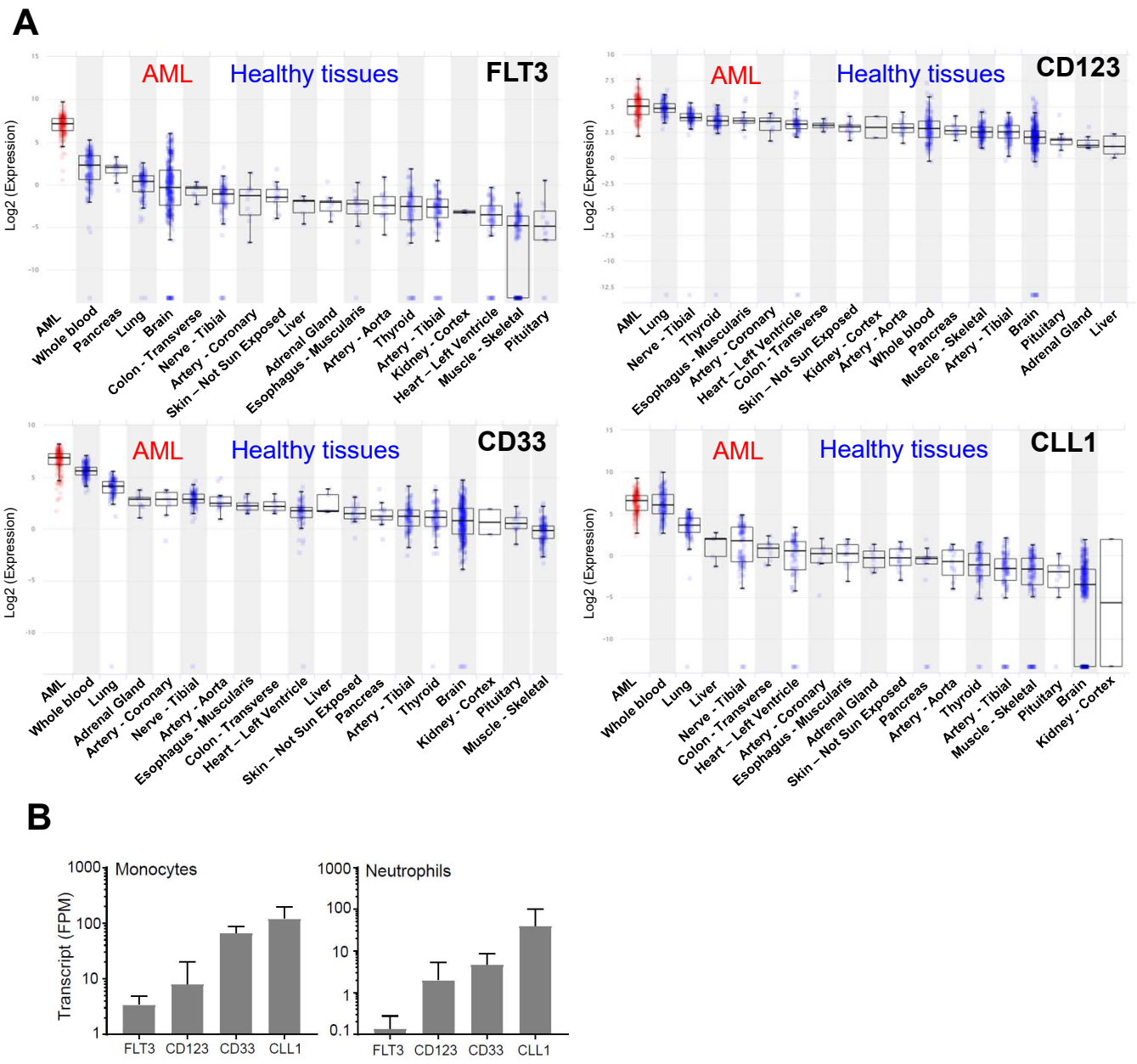

Figure S1. Gene expression profiles of FLT3, CD33, CLL1 and CD123 in AML and various major healthy tissues. (A) Comparison of gene expression (RNA-seq) for FLT3, CD123, CD33, and CLL1 from publicly available gene expression databases. AML gene expression was imported from The Cancer Genome Atlas (TCGA). Gene expression from 18 major healthy tissues was imported from Genotype-Tissue Expression data (GTEx) portal. (B) Gene expression analysis (RNA-seq) from sorted immune cells imported from the BLUEPRINT Data Analysis Portal. FLT3 expression in monocytes and neutrophils was the lowest compared to three other AML targets.

Figure S2

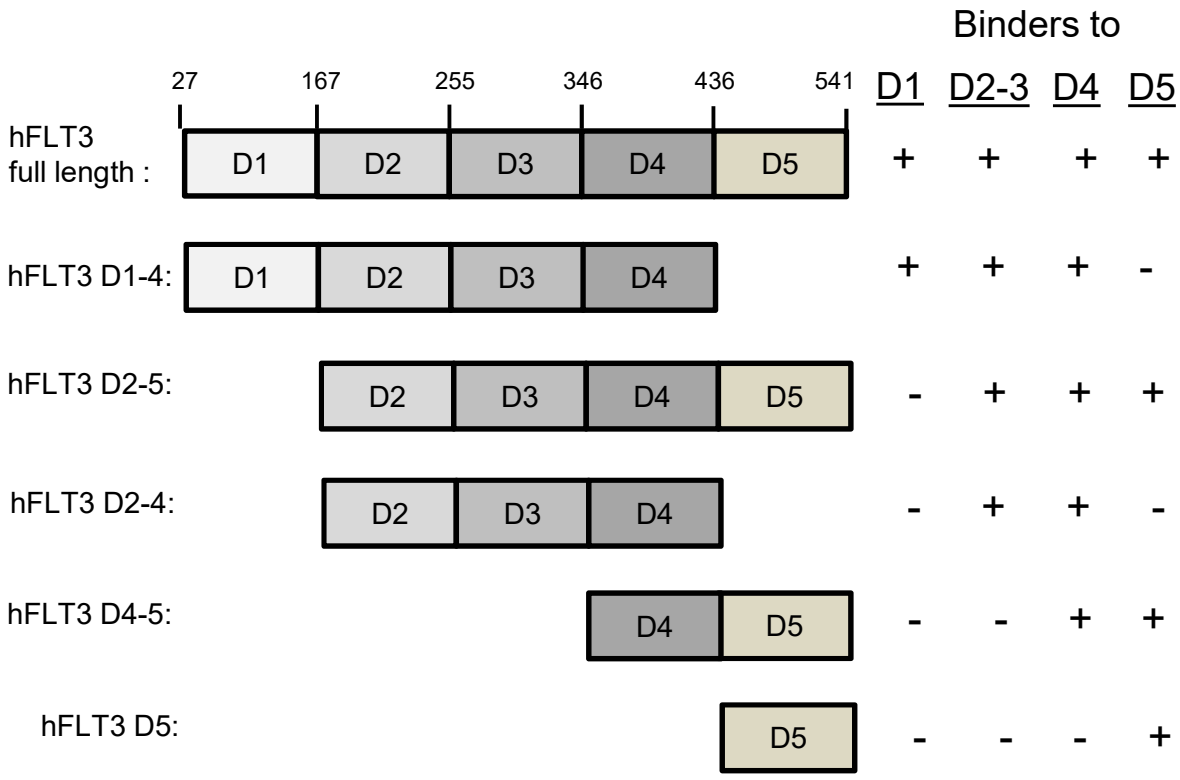

Figure S2. Schematic representation of the recombinant full length FLT3 and various truncated forms of FLT3. Recombinant his-tagged full length and truncated FLT3 proteins were expressed in HEK293 cells and purified using Nickel affinity chromatography. The recombinant proteins were used to map the binding domains of anti-FLT3 antibodies using ELISA. D1, D4 and D5 binders could be straightforwardly identified from the ELISA. Recombinant FLT3 D2 and D3 could not be expressed without the other domain, therefore binders against D2 and D3 could not be segregated into individual domain binders using these truncation variants. These clones were labeled as D2-D3 binders. “+” denotes positive binding in ELISA; “-” denotes no binding in ELISA.

Figure S3

A

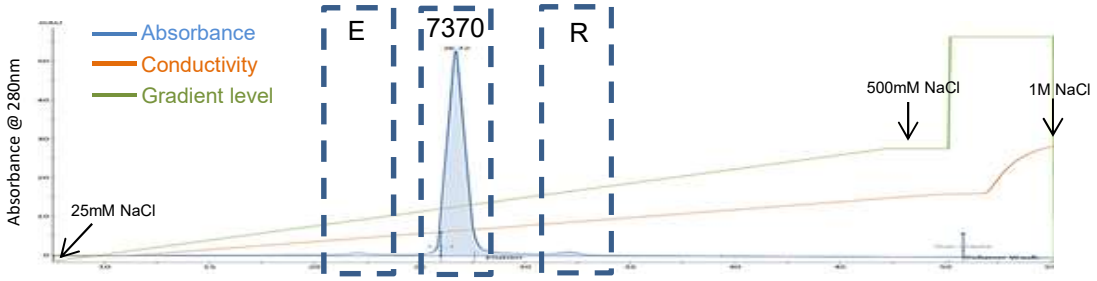

B

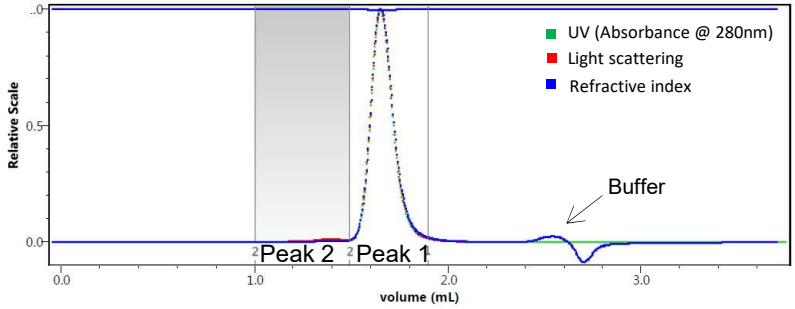

C

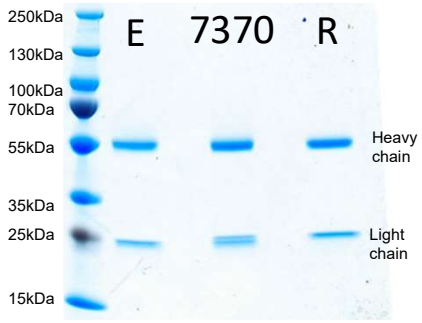

D

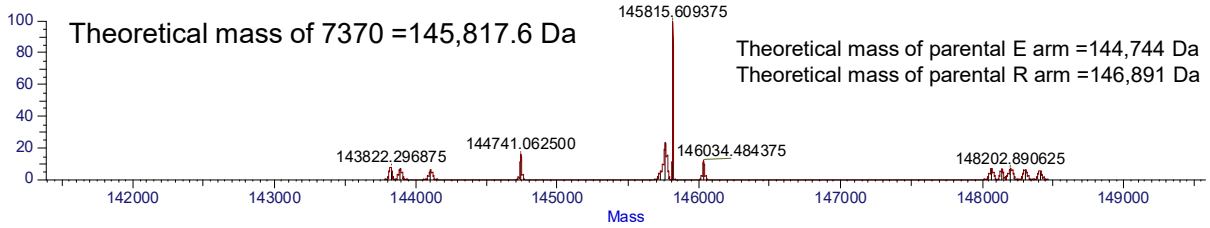

E

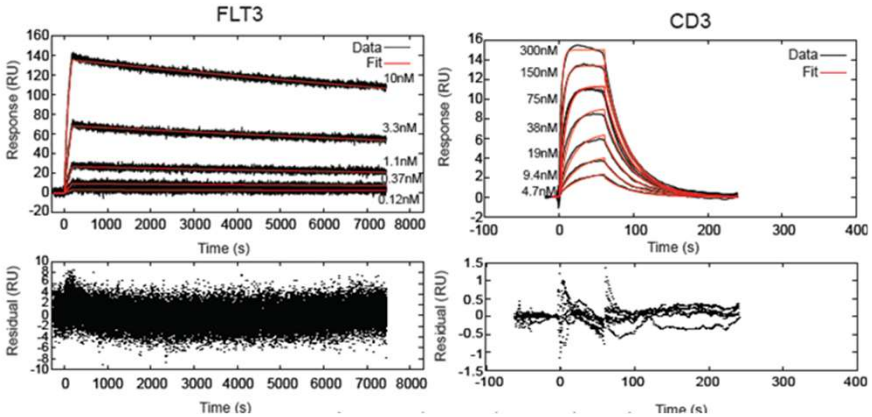

	k_{on} ($x10^5$ $M^{-1}s^{-1}$)	k_{off} ($x10^{-5}$ s^{-1})	K_D (nM)
Human FLT3	6.5	3.2	**0.049**
Human CD3	12	3000	**27**
Cyno CD3	9.6	2800	**29**

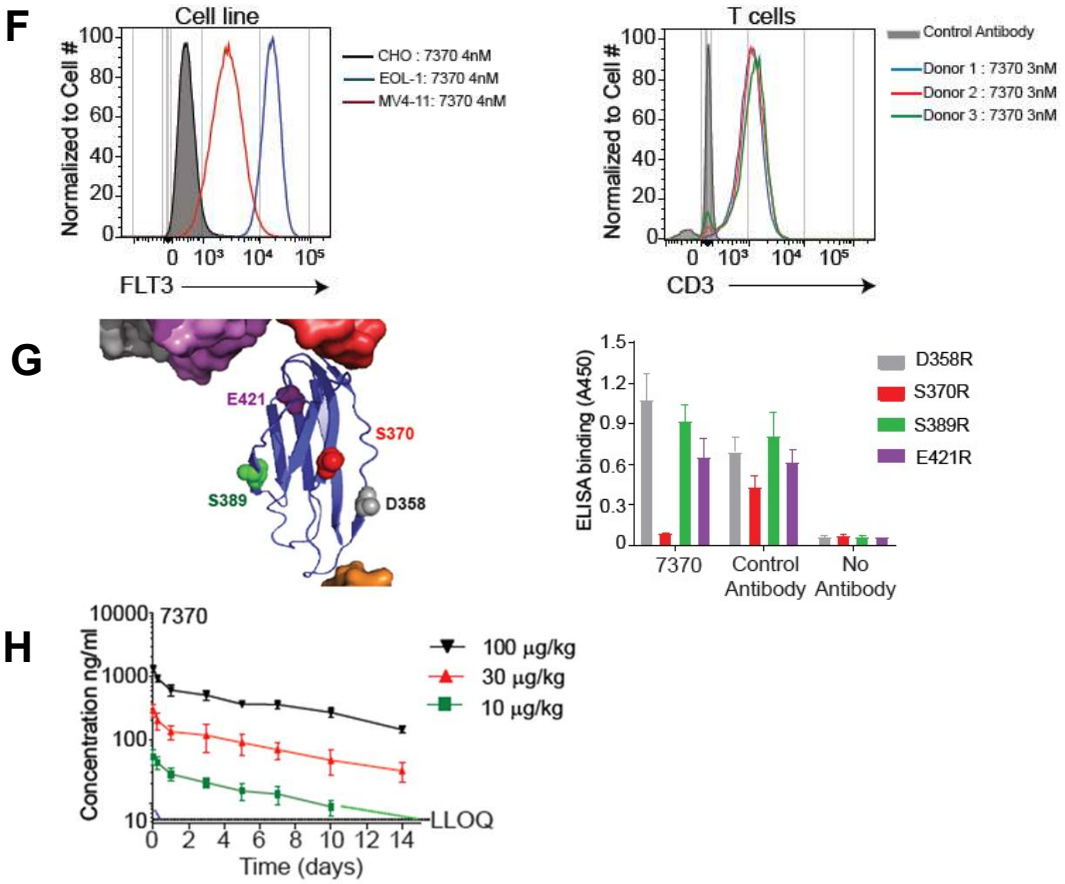

Figure S3. Properties of 7370 FLT3-CD3 bispecific IgG. (A) Analytical ion-exchange chromatographic analysis for heterodimer detection. Purified 7370 was analyzed using a MonoS column. (GE Healthcare). Running condition was 20mM MES buffer pH 5.4 with increasing NaCl concentration from 25mM to 1M. The heterodimeric bispecific antibody represent >95% of the injected materials. (B) Size-exclusion chromatographic and multi-angle light scattering (SEC-MALS) analysis. 7370 (Peak1) was determined to be 99% monomeric by SEC with an average molar mass of 1.49×10^5 (+ 0.061%) g/mol by light scattering. (C) Purity analysis of 7370 and parental E & R arms in reducing protein gel electrophoresis. (D) Intact mass analysis of 7370 by mass spectrometry. The experimental mass of 7370 matched well to the theoretical mass of 7370. (E) The dissociation constant of 7370 against recombinant human FLT3 and CD3εδ heterodimer. Binding at 37°C was determined using surface plasmon resonance. Binding sensorgram from 1 representative experiment out of 3 independent experiments was shown. Binding affinity of 7370 against recombinant cyno CD3εδ heterodimer is also summarized in the table. (F) Binding of 7370 to human T cells and AML cell lines, EOL-1 and MV4-11 by flow cytometry. CHO was used as the negative control cell line. (G) Binding of 7370 to arginine substitution variants at various human FLT3 domain 4 positions. Four residues (D358, S370, S389 and E421) at spatially distinct regions of FLT3 D4 (shown as blue ribbon) were selected to generate single-point arginine substitution variants. Binding of antibodies against FLT3 D4 arginine variants coated on plate was determined using ELISA. (H) Pharmacokinetic study of a single injection of 7370 in MOLM-13-bearing NSG mice. Three different groups of mice were injected IV with 10, 30 and 100 µg/kg of 7370. Serum concentration of 7370 was monitored over time. N=3 mice per group; LLOQ – lower limit of quantitation.

Figure S4

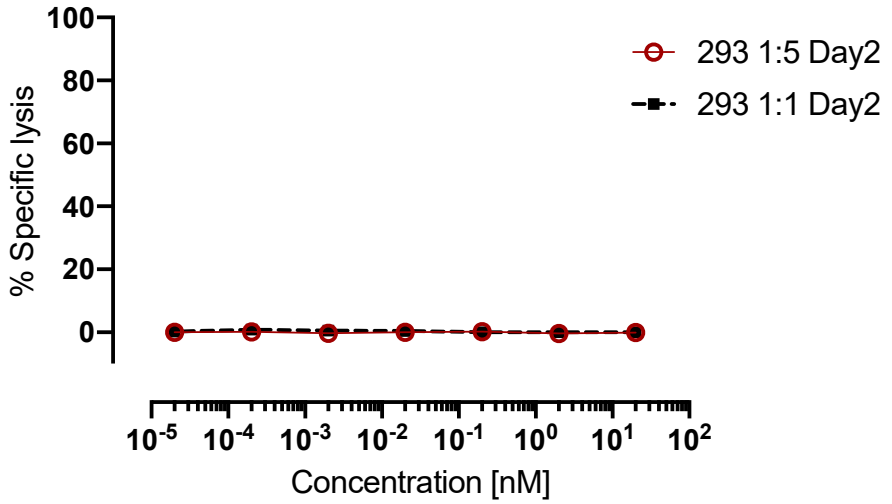

Figure S4. 7370 did not exhibit cytotoxicity against a FLT3-negative cell line FLT3-negative 293 cells were incubated with T cells isolated from one healthy human donor at E:T ratio of 1:1 and 1:5 in the presence of various concentrations of 7370. Cytotoxicity was determined after 2 days.

Figure S5

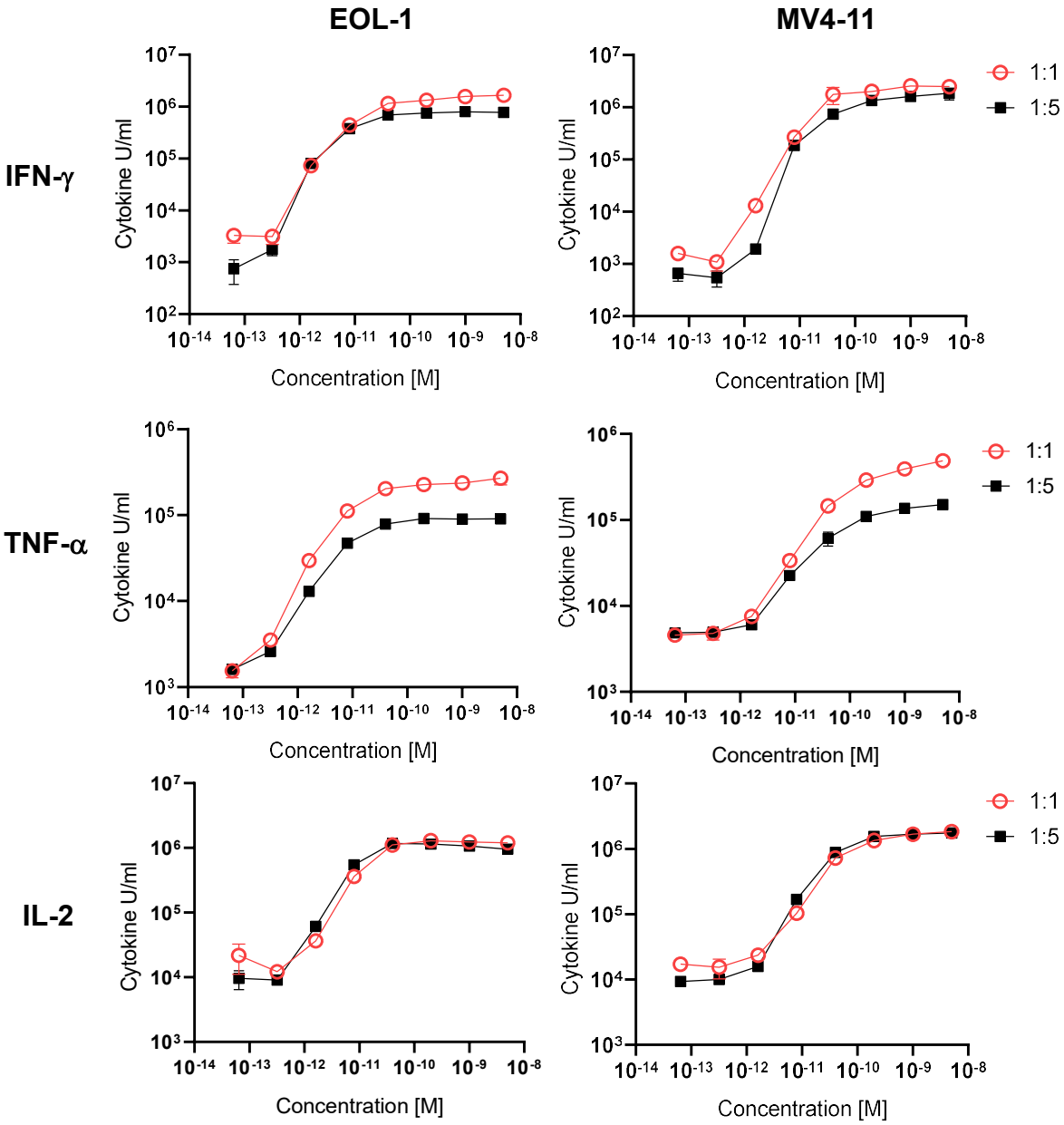

Figure S5. IFN-γ, TNF-α, and IL-2 cytokine secretion is induced by 7370. Measurement of the three cytokines in the supernatant 1 days after coculture of healthy donor human T cells with 7370 in the presence of EOL-1 (left) or MV4-11 (right) at two different E:T ratios (1:1 and 1:5). Human T cells were isolated from one human donor. Data shown is the average and error from three replicates.

Figure S6

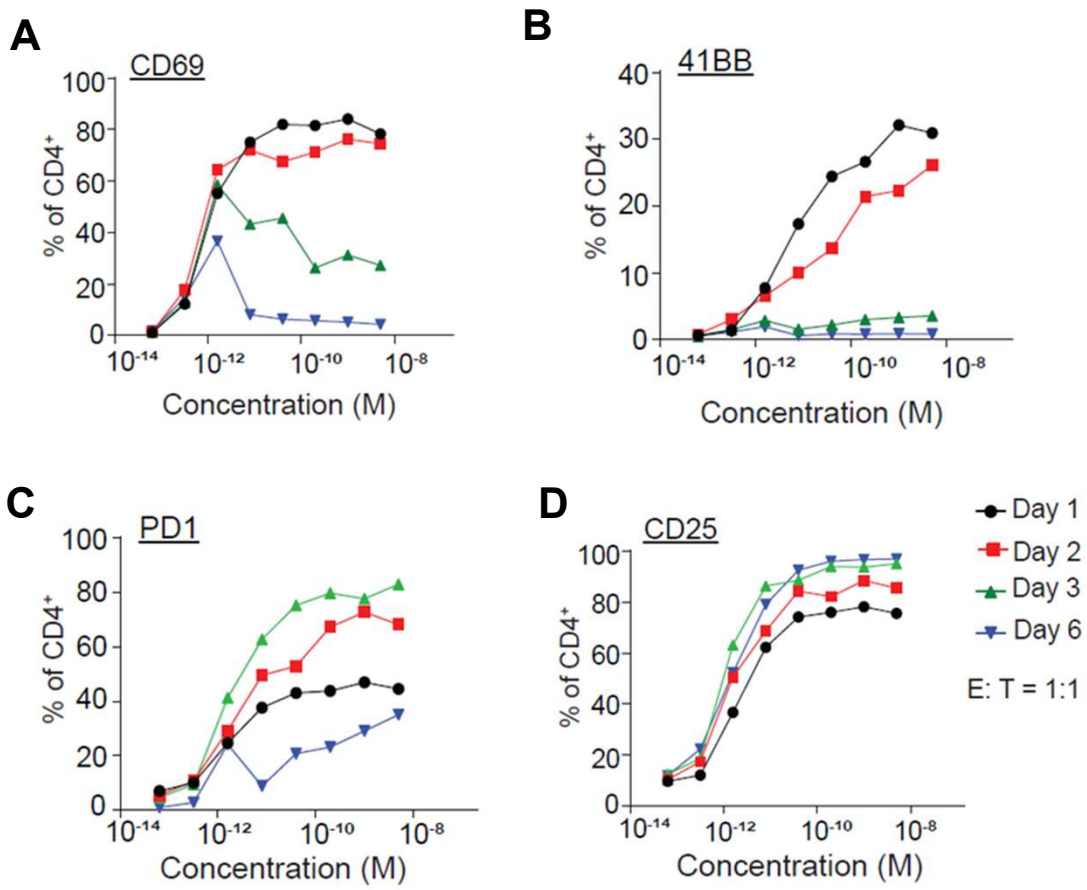

Figure S6. CD4⁺ T cells are activated following exposure to EOL-1 in the presence of 7370. Change in activation markers for CD4⁺ T cells over time**.** EOL-1 cells were co-cultured with human T cells (E:T of 1:1) and 7370 at indicated concentrations. CD4⁺ T cells were analyzed by flow cytometry for the kinetics of expression of activation markers at 1, 2, 3 and 6 following the start of co-culture. Activation markers CD69 (A), 41BB (B), PD1 (C) and CD25 (D) of CD4 T cells are shown as a function of bispecific concentration. Human T cells were isolated from one human donor. Each data point represents one measurement.

Figure S7

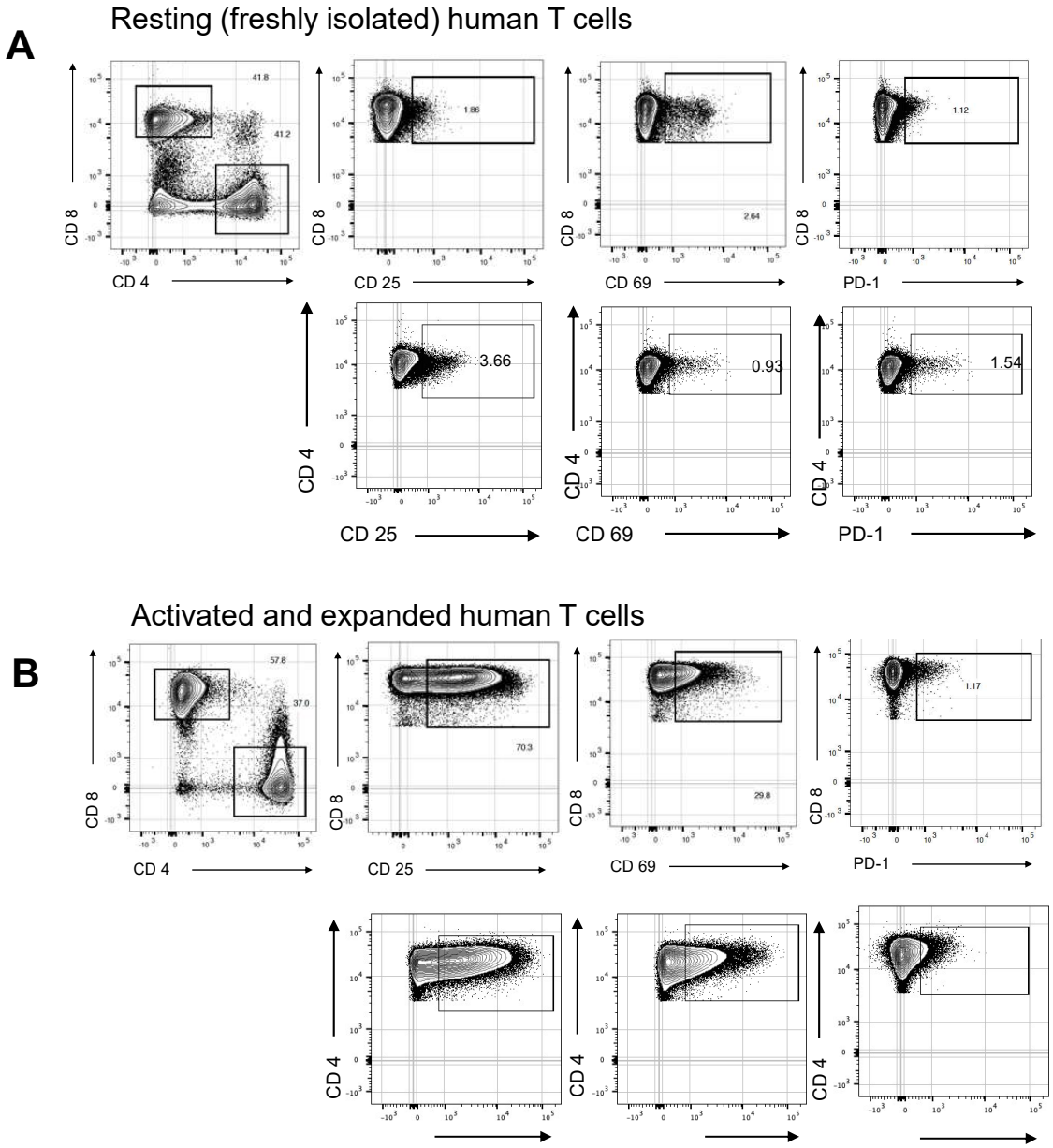

Figure S7. Immune phenotype of T cells injected into NSG mice. Cryopreserved T cells isolated from a representative human donor were thawed and analyzed for the expression of CD4, CD8, CD25, CD69, and PD1 immediately after thawing (A) or 11 days after activation with anti-CD3 and anti-CD28 antibodies and expansion in IL-2 (B).

Figure S8

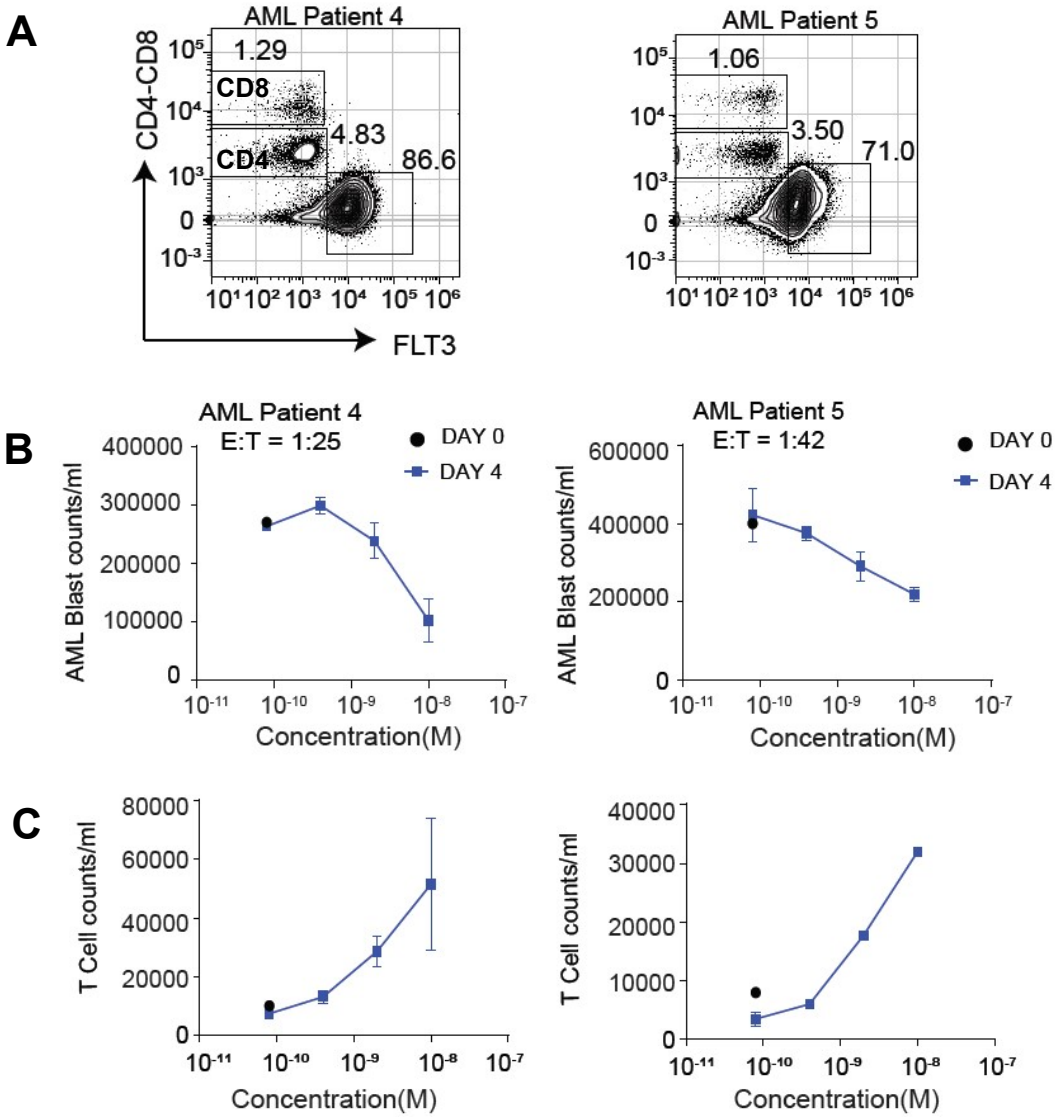

Figure S8: Autologous T cells proliferate and kill AML blasts in the presence of 7370 in a dose-dependent manner (A) Expression of FLT3 (x-axis) and CD4 and CD8 (y-axis) in PBMCs from two AML patients. Percent of CD4+ (middle left gate), CD8+ (upper left gate) and FLT3+ cells (bottom right gate) is depicted. FLT3 expression was detected only in $CD45^{low}$ blasts. (B-C) AML blast (B) and T cell counts (C) in patients 4 and 5 after 4 days of culture with 7370. Black dot on the graphs denotes the cell count at Day 0 before the addition of 7370. Each measurement is an average of three technical replicates.

Figure S9

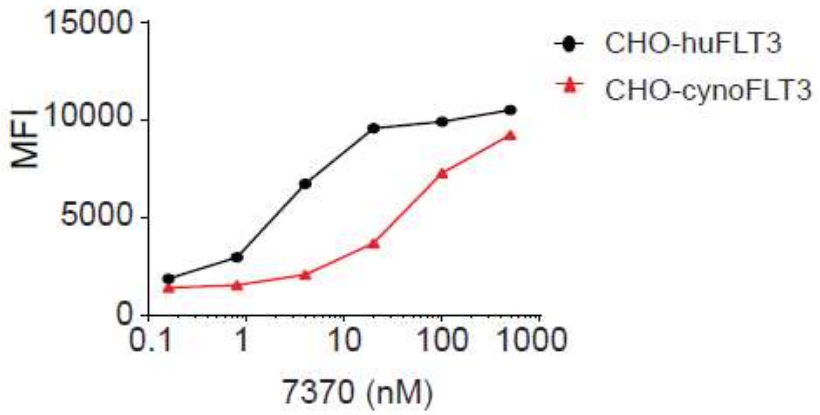

Figure S9: Binding EC_{50} of 7370 to cyno FLT3 is ~13 fold lower than that of human FLT3. Binding affinity using recombinant cynomolgus FLT3 protein could not be reliably measured due to the instability and aggregation of the purified protein (data not shown), so we tested the binding of 7370 on CHO cells expressing human (black line) or cynomolgus FLT3 (red line). Engineered cell lines were incubated with increasing concentrations of 7370 at 4°C. Binding of 7370 to the cells was analyzed by flow cytometry in two independent experiments. Each data point represents one measurement.

Figure S10

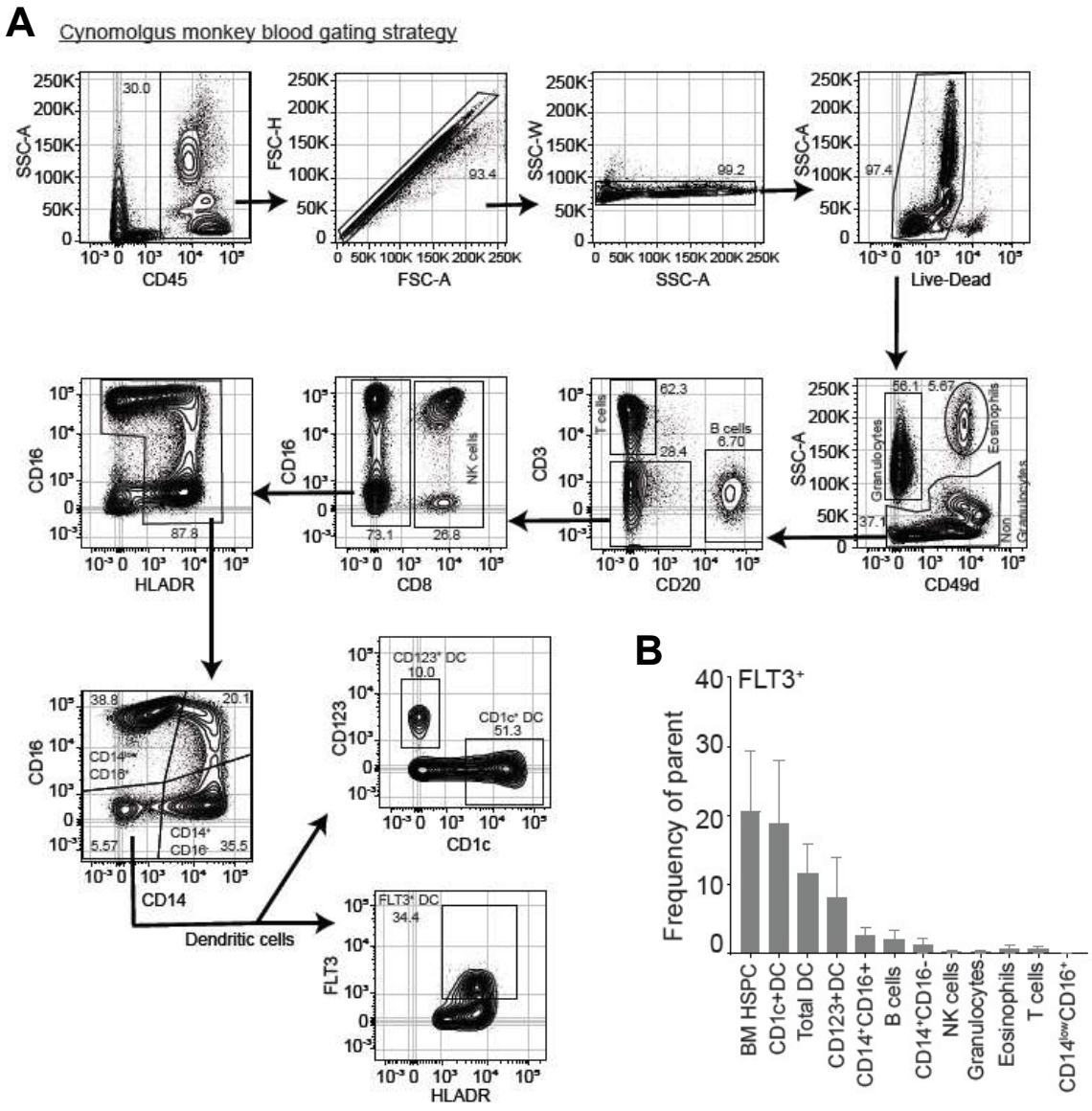

Figure S10: FLT3 expression in cynomolgus monkey blood immune cell subsets. (A) Flow cytometry gating strategy that identifies the following subsets from red blood cell-lysed whole blood is shown: eosinophils ($CD45^+CD49d^+SSC^{hi}$), granulocytes ($CD45^+CD49d^-SSC^{hi}$), T cells ($CD45^+SSC^{low}CD3^+CD20^-$), B cells ($CD45^+SSC^{low}CD3^-CD20^+$), NK cells ($CD45^+SSC^{low}CD3^-CD20^-CD16^{+/-}CD8^+$), classical monocytes ($CD45^+SSC^{low}CD3^-CD20^-CD8^-CD14^+CD16^-$), inflammatory monocytes ($CD45^+SSC^{low}CD3^-CD20^-CD8^-CD14^+CD16^+$), nonclassical monocytes ($CD45^+SSC^{low}CD3^-CD20^-CD8^-CD14^{low}CD16^+$), and dendritic cells ($CD45^+SSC^{low}CD3^-CD20^-CD8^-HLADR^+CD14^-CD16^-$). Two subsets of dendritic cells were additionally identified CD1c+ (myeloid) and CD123+ (plasmacytoid). FLT3 expression in total dendritic cells is depicted. (B) Percentage of FLT3-expressing cells in the indicated blood immune cell subsets. Bone marrow HSPCs (CD34+CD38+) are also depicted for comparison. N=6 monkeys. FLT3 was detected by BV10 antibody as 4G8 does not cross-react to cynomolgous FLT3.

Figure S11

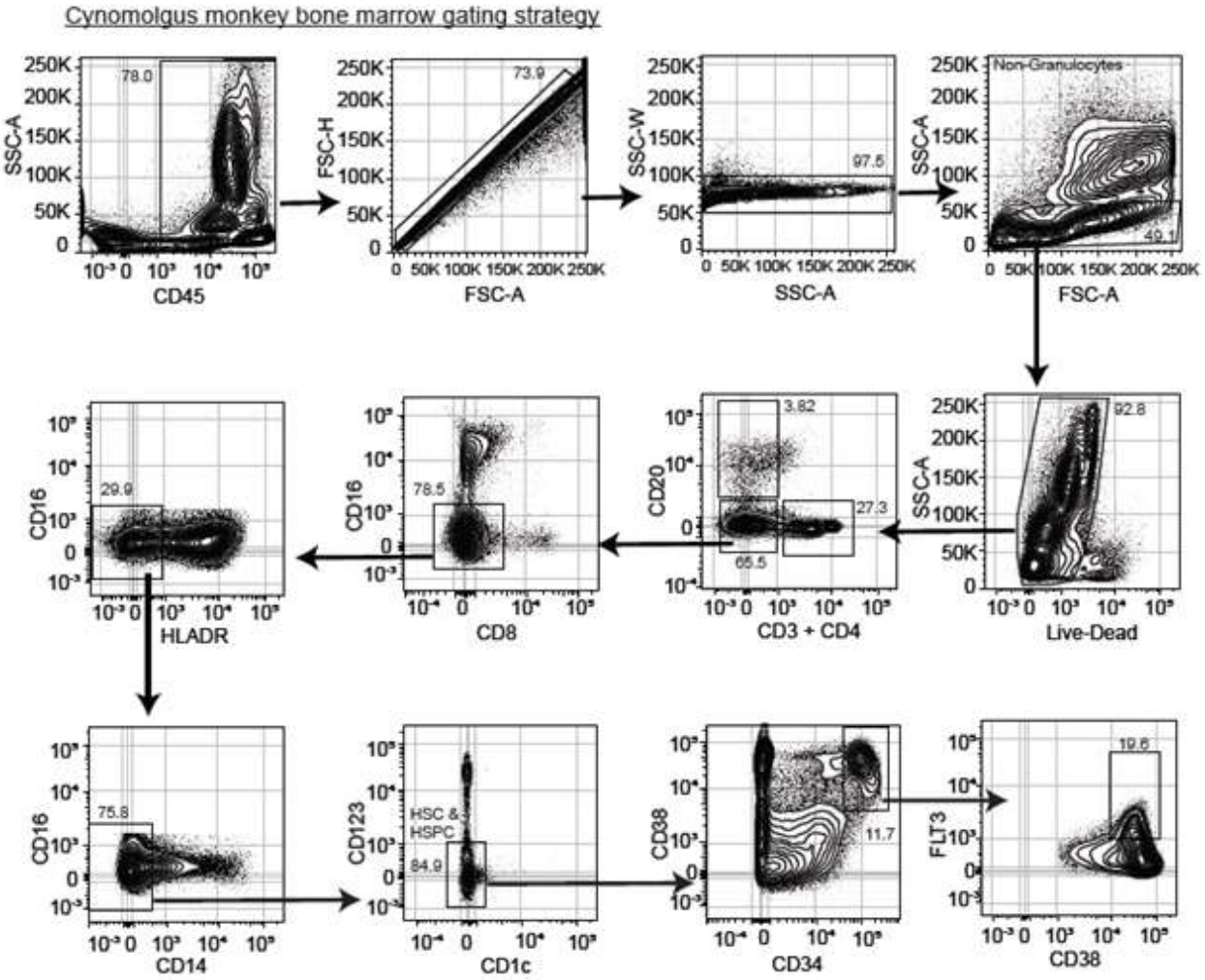

Figure S11: FLT3 expression in cynomolgus monkey bone marrow. Flow cytometry gating strategy that identifies $CD34^{+}CD38^{+}$ HSPCs from red blood cell-lysed bone marrow is shown. Identified $CD34^{+}CD38^{+}$ HSPCs were $CD45^{+}SSC^{low}$ but negative for the following lineage-specific markers: CD3, CD20, CD4, CD8, CD16, HLADR, CD14, CD123, CD1c. The expression of FLT3 in the $CD34^{+}CD38^{+}$ HSPC subset is shown. FLT3 was also expressed in bone marrow dendritic cells identified as in Supplementary Figure 6 (data not shown). Expression pattern of FLT3 in other differentiated immune subsets in the bone marrow was similar to that in the blood (data not shown).

Figure S12

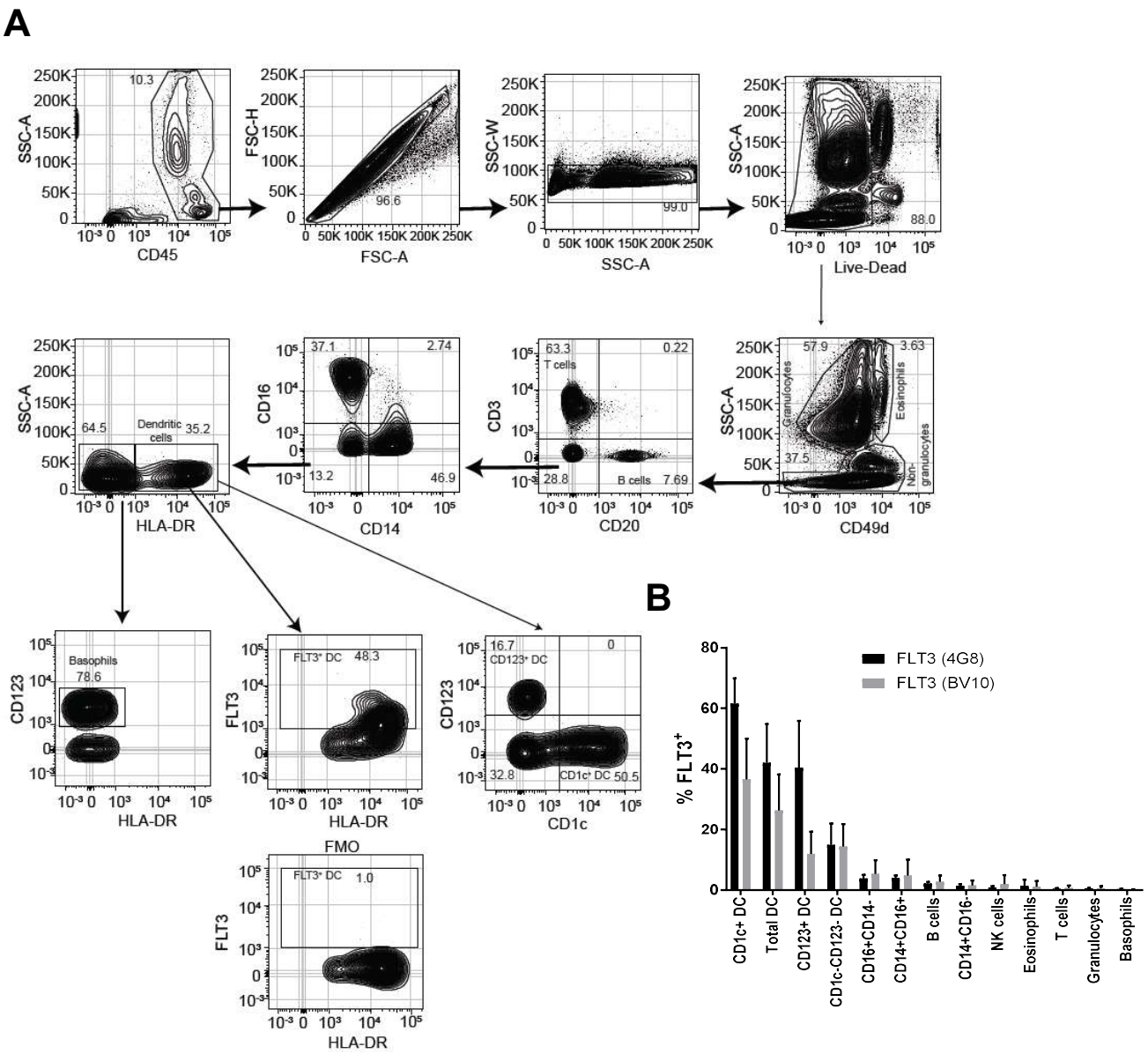

Figure S12: FLT3 expression in human blood immune cell subsets. (A) Flow cytometry gating strategy that identifies the following subsets from red blood cell-lysed whole blood is shown: eosinophils ($CD45^+CD49d^+SSChi$), granulocytes ($CD45^+CD49d^-SSChi$), T cells ($CD45^+SSC^{low}CD3^+CD20^-$), B cells ($CD45^+SSC^{low}CD3^-CD20^+$), classical monocytes ($CD45^+SSC^{low}CD3^-CD20^-CD14^+CD16^-$), inflammatory monocytes ($CD45^+SSC^{low}CD3^-CD20^-CD14^+CD16^+$), nonclassical monocytes ($CD45^+SSC^{low}CD3^-CD20^-CD14^-CD16^+HLADR^+$), NK cells ($CD45^+SSC^{low}CD3^-CD20^-CD14^-CD16^+HLADR^-$), and dendritic cells ($CD45^+SSC^{low}CD3^-CD20^-CD14^-CD16^-HLADR^+$). $CD1c^+$, $CD123^+$, and $CD1c^-CD123^-$ subsets are also indicated. FLT3 expression in total dendritic cells is shown (control with no antibody is included to show how $FLT3^+$ cells were identified). (B) Percentage of FLT3-expressing cells in the indicated blood immune cell subsets of 4 healthy donors as measured by staining with 4G8 or BV10 antibody.

Figure S13

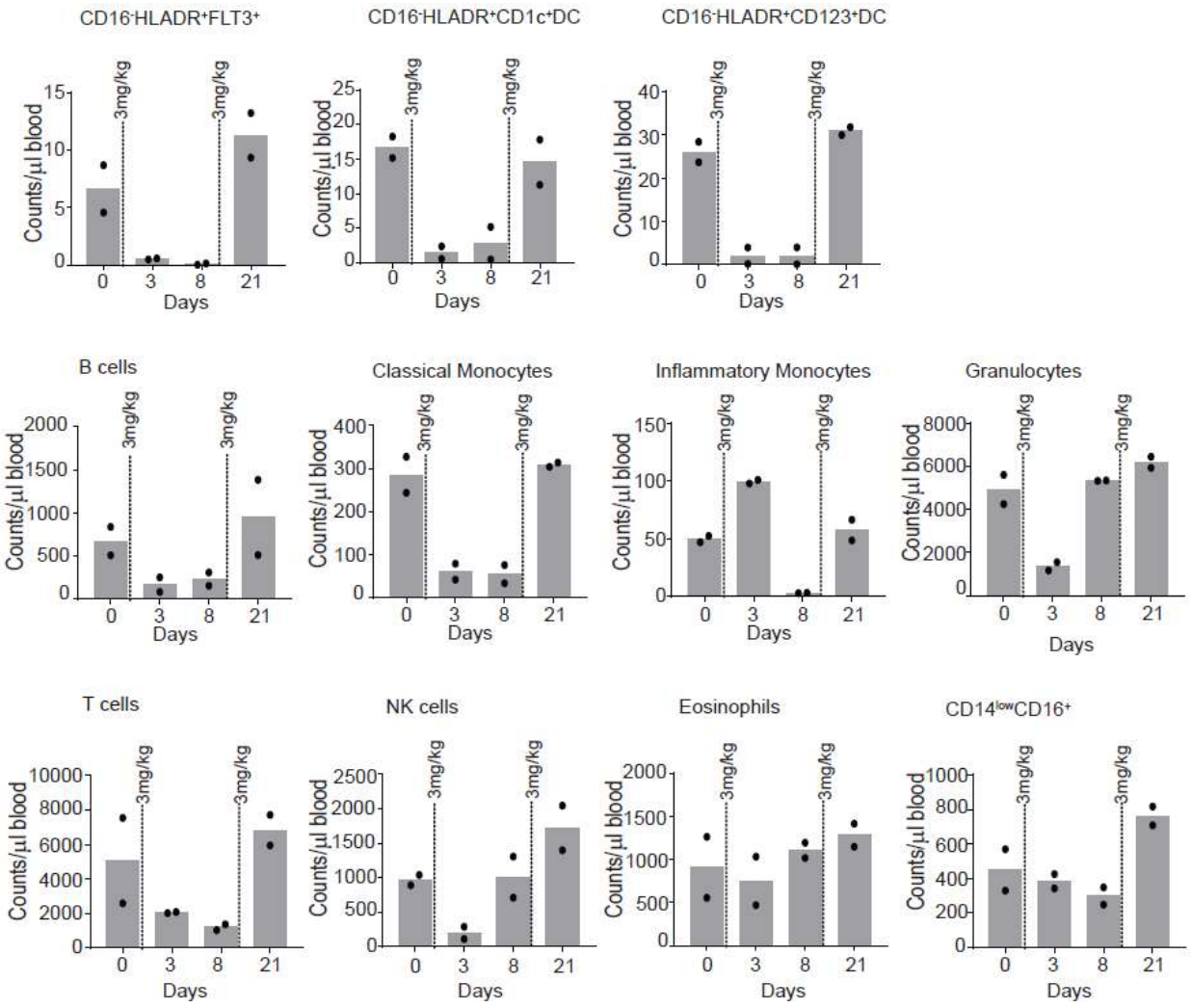

Figure S13: 7370 is well tolerated and exhibits on-target efficacy in peripheral blood of cynomolgus monkeys. Cell counts per microliter in the blood of cynomolgus monkeys treated with 7370 (monkeys “Treated 3” and “Treated 4” as depicted in Figure 5A). Immune cell subsets were identified as shown in Supplementary Figure 6. Cell counts were determined using counting beads.

Figure S14

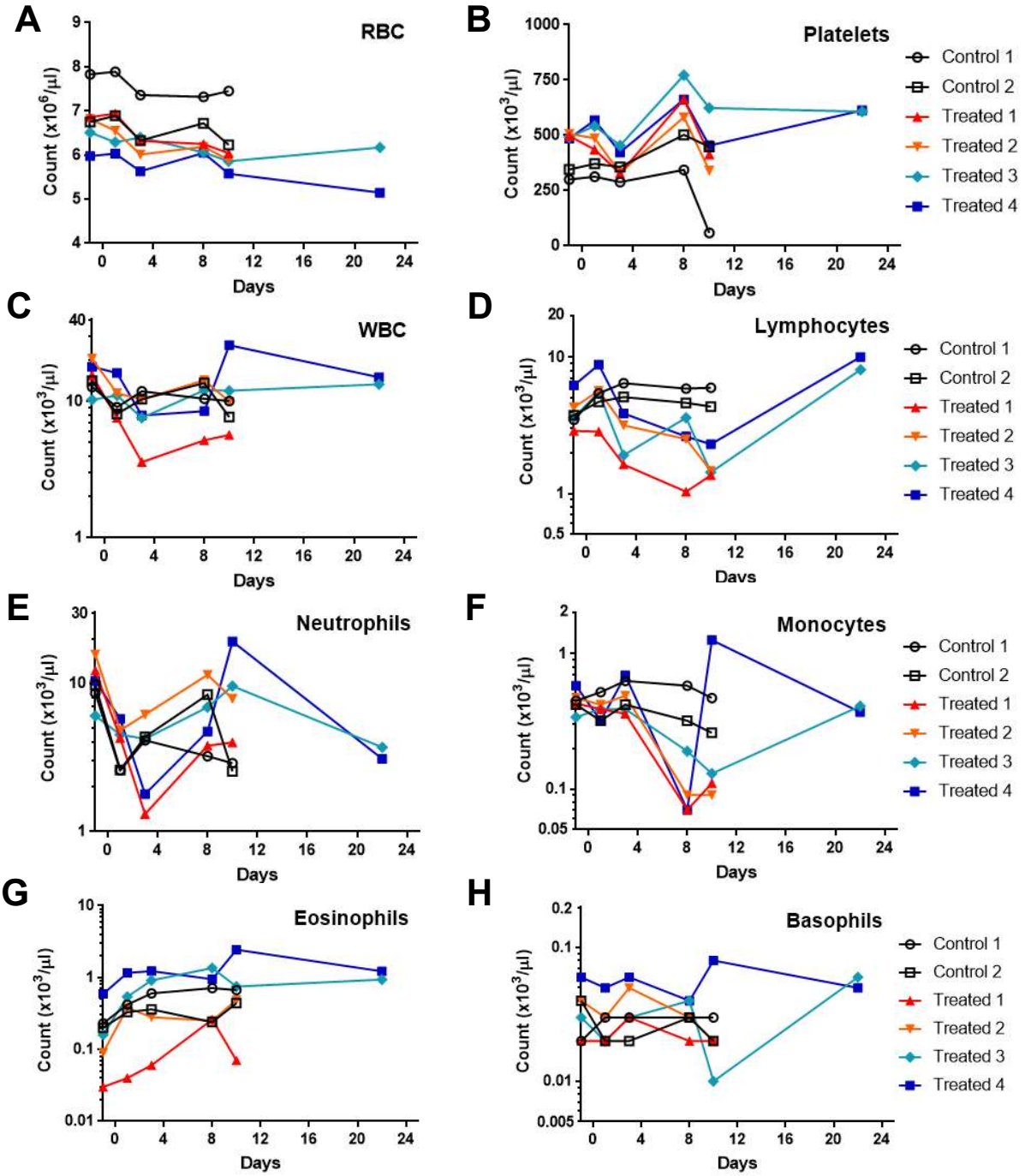

Figure S14: Peripheral immune cell populations in Cynomolgus monkeys based on hematology counts. Six monkeys were treated with PBS (Control 1 and 2) or 2 doses of 7370 at 3mg/kg at days 1 and 8 (Treated 1-4) (see Figure 5A). Standard hematology was performed at the indicated time points. Day -1 and day 1 samples were collected before the first injection of 7370. Day 8 samples were collected before the second dose of 7370. Results for (A) red blood cell (RBC), (B) platelets, (C) white blood cells (WBC), (D) lymphocytes, (E) neutrophils, (F) monocytes, (G) eosinophils and (H) basophils are shown.

Figure S15

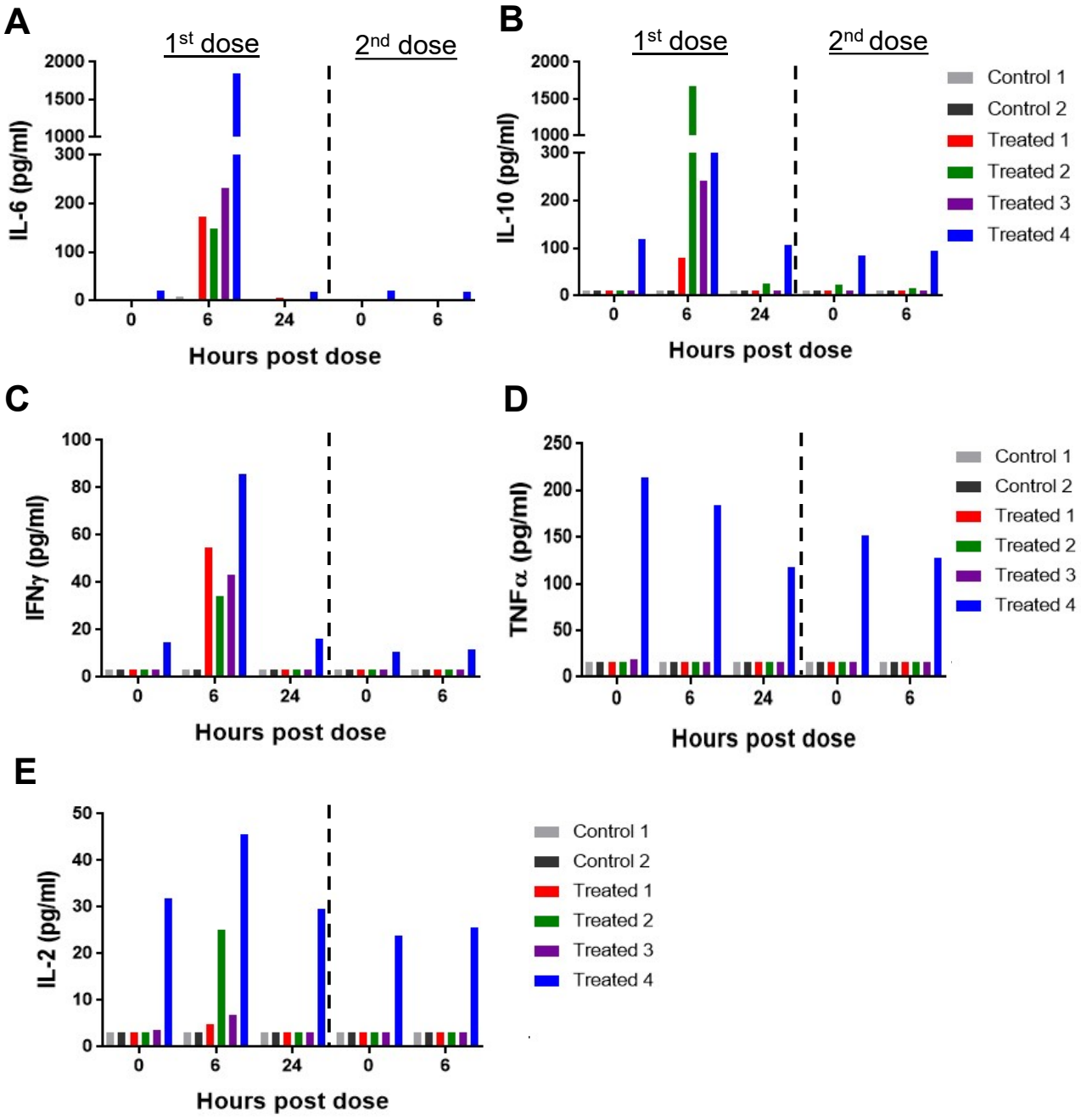

Figure S15: Serum cytokines in cynomolgus monkeys after treatment with 7370. Six monkeys were treated with PBS (Control 1 and 2) or 2 doses of 7370 at 3mg/kg at days 1 and 8 (Treated 1-4) (see Figure 5A). Serum levels for selected cytokines were monitored pre-dose (0), 6 and 24 hours post first dose, before (0) and 6 hours post second dose. Serum concentration of (A) IL-6, (B) IL-10, (C) IFNγ, (D) TNFα, and (E) IL-2 are shown. Compared to the other monkeys, treated monkey 4 had higher pre-dose levels for all evaluated cytokines, and had much higher IL-6 levels post first dose.

Supplementary methods:

Cell binding assays of 7370

FLT3-negative CHO cells, CHO cells engineered to express human or cynomolgus FLT3, EOL-1 and MV4-11 cells, and human T cells were assessed for binding to 7370. 200,000 cells were plated and incubated with 7370 at concentrations 500nM to 0.0016nM (fivefold serial dilution) for 20 minutes at 4°C. Cells were washed, stained with F_{ab} fragment of goat anti-human IgG-F_c antibody and analyzed on a LSRII with FACS Diva software (BD Biosciences).

Cytokine detection in supernatants of T cell-AML cell line co-cultures

In a 96 well U bottom plate, AML cell lines (EOL-1, and MV4-11) were co-cultured with human T cells under different concentrations of 7370 in E:T ratios of 1:1 and 1:5 for 24hrs. Supernatants of the co-cultures at 24hrs were harvested, diluted at 1:50 with the diluent provided in the MSD kit (Mesoscale discovery kit) and analyzed for cytokines (IL2, IFNγ and TNFα) on MSD plates as per manufacturers protocol.

Detection of 7370 in mouse serum

Mouse anti-hCD3 Id antibody Biotin captured onto streptavidin-coated beads on the affinity capture column of the Gyrolab Bioaffy microstructure was used to bind 7370. Bound 7370 was detected with Alexa 647-labeled goat anti-human IgG (H+L). A fluorescent signal on the column, representative of the amount of bound 7370, allows for visualization of the antibody. Response Units are read by the Gyrolab instrument at 1% Photomultiplier tube (PMT) setting. Sample concentrations are determined by interpolation from a standard curve that is fit using a 5-parameter logistic curve fit with $1/y^2$ response weighting. The standard points in 2.5% K_2 EDTA mouse plasma ranged from 0.057 ng/mL to 150 ng/mL. The range of quantitation in mouse plasma was 5.45 ng/mL to 2500 ng/mL.

Serum cytokine detection

IL-2, IL-6, IL-10, IFN-γ, and TNF-α were simultaneously quantified in serum samples using the Millipore Milliplex MAP Non-Human Primate Cytokine Magnetic Bead Panel reagent kit (cat. #PRCYTOMAG-40K). Limits of detection for the cytokine assays are 3.20 pg/mL for IL-2, IL6, and IFN-γ, 12.20 pg/mL for IL-10, and 16.00 pg/mL for TNF-α.